STATE OF ALASKA

DEPARTMENT OF NATURAL RESOURCES

DIVISION OF GEOLOGICAL AND GEOPHYSICAL SURVEYS

John W. Katz — *Commissioner*

Geoffrey Haynes — *Deputy Commissioner*

Ross G. Schaff — *State Geologist*

November 1982

This is a preliminary publication of the Alaska Division of Geological and Geophysical Surveys and has not received final editing and review. The author will appreciate candid comments on the accuracy of the data and will welcome suggestions to improve the report.

Alaska Open-file Report 169

BEDROCK GEOLOGY AND PETROLOGY OF THE FAIRBANKS MINING DISTRICT, ALASKA

By
Robert B. Forbes

With contributions by
Florence R. Weber, Richard C. Swainbank,
Joe M. Britton, and James M. Brown

STATE OF ALASKA
Department of Natural Resources
DIVISION OF GEOLOGICAL & GEOPHYSICAL SURVEYS

According to Alaska Statute 41, the Alaska Division of Geological and Geophysical Surveys is charged with conducting 'geological and geophysical surveys to determine the potential of Alaska lands for production of metals, minerals, fuels, and geothermal resources; the locations and supplies of ground waters and construction materials; the potential geologic hazards to buildings, roads, bridges, and other installations and structures; and shall conduct other surveys and investigations as will advance knowledge of the geology of Alaska.'

In addition, the Division shall collect, evaluate, and publish data on the underground, surface, and coastal waters of the state. It shall also process and file data from water-well-drilling logs.

DGGS performs numerous functions, all under the direction of the State Geologist---resource investigations (including mineral, petroleum, and water resources), geologic-hazard and geochemical investigations, and information services.

Administrative functions are performed under the direction of the State Geologist, who maintains his office in Anchorage (3001 Porcupine Dr., 99501, ph 274-9681).

This report is for sale by DGGS for $1. It may be inspected at any of the four DGGS information offices: Alaska National Bank of the North Bldg., Geist Rd. and University Ave., Fairbanks; 3601 C St., Anchorage; 230 So. Franklin St., Juneau; and the State Office Bldg., Ketchikan. Mail orders should be addressed to DGGS, P.O. Box 80007, College, AK 99708.

CONTENTS

	Page
Abstract	1
Introduction	2
The Fairbanks mining district	2
Mining history	3
Gold mining and production	3
Antimony and tungsten production	4
Previous work	4
Acknowledgments	5
Regional geology and tectonic history	5
The Yukon-Tanana metamorphic complex	5
Metamorphic and intrusive history	5
Age of parent rocks	7
Mesozoic sedimentary and volcanic rocks	7
Sedimentary rocks	7
Volcanic rocks	7
Tertiary sedimentary and volcanic rocks	7
Sedimentary rocks	7
Volcanic rocks	9
Quaternary volcanism and surficial deposits	9
Volcanic rocks	9
Glacial history	9
Alluvial and colluvial deposits	10
Permafrost	10
Regional tectonic history	10
Tectonic framework	10
Tectonics of the Yukon-Tanana crystalline block	12
Petrology of the metamorphic rocks	13
Regional metamorphic setting	13
Range in metamorphic facies and lithology	14
Distribution of facies and rock types	14
Greenschist-facies suite	15
Micaceous quartzites and quartz-mica schists	15
Pelitic schists	15
Feldspathic quartz-mica schists	15
Calc-magnesian schists	15
Marbles	17
Quartzite and slate	17
Amphibolite-facies suite	17
Micaceous quartzites and quartz-mica schists	17
Garnet-mica (pelitic) schists	17
Gneisses	17
Ortho-amphibolites	18
Para-amphibolites	20
Calc-magnesian schists	20
Marbles	20
Eclogite-facies terrane	20
Quartzites and micaceous quartzites	21
Pelitic schists	21

Page

Impure marbles..... 21
Eclogites and garnet amphibolites..... 21
Garnet-clinopyroxene rocks (eclogites)..... 22
Garnet-clinopyroxene-amphibole rocks..... 22
Garnet-amphibole rocks..... 23
Whole-rock analyses of rocks from the eclogite-facies terrane..... 23
Comparative chemical and normative composition of the eclogitic rocks..... 23
Sedimentary vs mafic igneous analogs..... 24
Proposed sedimentary parentage..... 24
Radiometric age relationships of the metamorphic rocks..... 29
Metamorphic facies vs apparent potassium-argon ages..... 29
Apparent whole-rock potassium-argon age relationships along the Elliott Highway..... 30
Previous potassium-argon and rubidium-strontium studies..... 31
Summary of radiometric age relations..... 31
Petrology of the granitic rocks..... 32
Distribution and cooling ages..... 32
Distribution..... 32
Crystallization age..... 32
Quartz diorite-granodiorite..... 32
Field relations..... 32
Petrography..... 34
Quartz monzonite..... 35
Field relations..... 35
Petrography..... 35
Altered granitic rocks..... 37
Whole-rock chemistry..... 37
Trace- and minor-element chemistry..... 40
Intrusive sequence and crystallization history..... 43
Contact metamorphic rocks..... 46
Gilmore Dome contact zone..... 46
Pedro Dome contact zone..... 46
Approach Hill contact zone..... 47
Petrology of the mafic igneous rocks..... 47
Basalts..... 47
Distribution and field relations..... 47
Petrology..... 47
Structural implications..... 48
Ultramafic rocks..... 50
Deformational history and structure..... 50
Large-amplitude folds..... 50
Northeast-trending anticlines and synclines..... 50
Northwest-trending recumbent folds and the 'Chatanika Window?'..... 50
Related microstructures..... 51
Small-amplitude folds and orientation..... 54
Stereographic analysis of structural elements in the lower and upper plates..... 54
Eclogite-bearing terrane as a window..... 54

Page

Ester Dome antiform..... 54
Faults..... 54
Pedro Dome thrust fault..... 54
Dome Creek fault..... 57
Clear Creek and Ruby Creek faults..... 57
Subsurface faulting and mineralization..... 57
Interpretation of geophysical-survey data..... 60
Airborne magnetometer surveys..... 60
Surface gravity and magnetometer surveys..... 60
Magnetometer profiles..... 60
Gravity profile..... 62
Mineralized zones and vein systems..... 62
Lode classification and distribution..... 62
Mineralogy of the gold-bearing lodes..... 62
Structural control..... 63
Syngenetic(?)-metals concentrations vs secondary mineralization... 63
Unanswered problems and recommendations for future work..... 64
Regional tectonics, structure, and geochronology..... 64
Geochronology and tectonics..... 64
Structure..... 64
Petrology..... 64
Eclogite-facies terrane..... 64
Amphibolite- vs greenschist-facies terranes..... 65
Granitic rocks..... 65
Mineral deposits..... 65
References cited..... 66

ILLUSTRATIONS

Figure 1a. Map showing location of the Fairbanks mining district..... 2
1b. Location map of the Fairbanks mining district, with four relevant 1:250,000 U.S. Geological Survey quadrangles.... 3
2. Regional geologic map of the Yukon-Tanana Upland..... 6
3. Tectonic map of the Yukon-Tanana Upland..... 11
4. FMA-CNK diagrams illustrating the compositional fields of Hawaiian theoleiites and alkali basalts, with plots of analyzed rocks from the Fairbanks mining district eclogite-facies terrane..... 25
5. ACF diagram illustrating the compositional fields of eclogites and mafic and ultramafic rocks, and plots of analyzed rocks from the Fairbanks mining district eclogite-facies terrane..... 26
6. ACF diagram showing the coincidence of eclogite rocks from the Fairbanks mining district and the compositional field of marly sedimentary rocks..... 27
7. FMA-CNK diagrams with plots illustrating the comparative composition of granitic rocks from the Fairbanks mining district, Alaska..... 41
8. Normative albite-orthoclase-anorthite diagram for analyzed granitic rocks in the Fairbanks mining district, Alaska..... 42

Page

9. TiO_2-SiO_2 variation diagram showing tholeiitic-basalt compositional provinces and plots for the analyzed basalts from Birch Hill and Millers Bluff..... 49
10. Structural style of folded rocks in the eclogite-bearing terrane, Fairbanks mining district, Alaska..... 52
11. Generalized structure sections across the eclogite-bearing terrane north of Fairbanks, Alaska..... 53
12a-b. Lower hemisphere stereographic plot of fold axes and 'b' mineral lineations in the Fairbanks mining district... 55
13. Generalized northwest-southeast structure section across southeast quadrant of Ester Dome, Alaska..... 56
14. Diagramatic south-southeast-north-northwest structure section from Gilmore Dome to the Chatanika River valley, Alaska..... 58
15. Attitudes of faults and mineralized veins in the Ester Dome and Pedro Dome-Cleary area, Fairbanks mining district, Alaska..... 59
16. Strike-frequency diagram of faults in the Pedro Dome area, Fairbanks mining district, Alaska..... 61

TABLES

Table 1. Potassium-argon ages of igneous and metamorphic rocks from the Fairbanks mining district, Alaska..... 8
2. Approximate modes of representative rock types from greenschist-facies terrane, Fairbanks mining district, Alaska..... 16
3. Representative modes of gneissic rocks from the Fairbanks mining district, Alaska..... 18
4. Whole-rock chemical analyses and CIPW norms of metamorphic rocks from the eclogite-facies terrane, Fairbanks mining district, Alaska..... 19
5. Modes of analyzed rocks from the eclogite-facies terrane, Fairbanks mining district, Alaska..... 28
6. Apparent potassium-argon ages of rocks from the Elliott Highway traverse, Fairbanks mining district, Alaska.... 30
7. Radiometric ages of granitic rocks from the Fairbanks, Circle, Livengood, and Big Delta Quadrangles, Alaska... 33
8. Modes of representative specimens of quartz diorite-granodiorite and quartz monzonite from the Fairbanks mining district, Alaska..... 36
9. Whole-rock analyses of granitic rocks from the Fairbanks mining district, Alaska..... 38
10. Igneous norms for chemically analyzed granitic rocks from the Fairbanks mining district, Alaska..... 39
11. Chemical and mineralogical parameters for the discrimination of 'S' vs 'I' granite types applied to analyzed granitic rocks from the Fairbanks mining district, Alaska..... 43
12. Spectrographic analyses of representative samples from the Pedro Dome plutons, Fairbanks mining district, Alaska.. 44

Page

13. Chemical analyses of Fairbanks mining district basalts..... 48
14. Modal analyses of basalts from the Fairbanks mining district, Alaska..... 48

ABSTRACT

Bedrock of the Fairbanks mining district is composed of metamorphic rocks assigned to the Yukon-Tanana metamorphic complex. Synkinematically metamorphosed rocks range from greenschist to amphibolite facies. The eclogite-bearing sequence is confined to a fault-bounded terrane or 'window' surrounded and tectonically overlain by an upper plate of greenschist-facies rocks. Amphibolite-facies metamorphic rocks tend to occur along northeast-trending synforms, and although the eclogite- and amphibolite-facies rocks may belong to a common terrane or lower plate, structural relations are as yet unclear.

The greenschist-facies terrane is dominated by quartz-mica schists and micaceous quartzites, with subordinate feldspathic schists, greenschists, calc-magnesian schists, and marbles. Amphibolite-facies sequences are characterized by amphibolites and garnet-mica schists with subordinate gneisses and marbles. The eclogite-bearing terrane is dominated by eclogitic rocks, garnet amphibolites, and black micaceous quartzites, with subordinate diopside marbles and garnet-mica schists.

The structural style of the eclogite-bearing terrane is defined by large-scale isoclinal recumbent folds with northwest-trending axes that have been refolded into northeast-trending synforms and antiforms.

Structures in the greenschist- and amphibolite-facies terranes are dominated by the northeast-trending structures, but small-scale, isoclinal-recumbent folds and discordant relations between earlier 'b' mineral lineations and northeast-trending fold axes suggest an earlier deformational episode.

Granitic plutons with compositions ranging from biotite granite and quartz monzonite to biotite-hornblende granodiorite and quartz diorite were intruded into the metamorphic host rocks during Cretaceous time. The Pedro and Gilmore Dome plutons have an elongate outcrop geometry that parallels the axial trace of the two dominant northeast-trending antiforms, suggesting structural control during emplacement.

Host metamorphic rocks are hornfelsed and upgraded near intrusive contacts. Calc-magnesian rocks have reacted to produce 'skarn' assemblages that are associated with tungsten and possible tin concentrations in the district.

Granitic dikes, the hypabyssal equivalent of the quartz-monzonitic plutonic rocks, are often sheared and mineralized in the Cleary-Pedro area. Quartz veinlets associated with brecciated and/or sheared dikes, and plutons frequently contain anomalous concentrations of gold.

Stained and leached(?) feldspathic schists also contain anomalous heavy-metals concentrations in the axial zones of the Pedro-Cleary and Ester Dome areas.

Metalliferous quartz lodes were emplaced along avenues created by selected fracture, joint, and fault systems during a time interval coincident with the emplacement of the granitic plutons.

Radiometric age data indicate that the parental sedimentary rocks (protolith) in the district were probably of Precambrian and/or early Paleozoic age, and that the earliest metamorphic event occurred in late Precambrian to early Paleozoic time. A second thermal pulse seems to have occurred in Jurassic time, followed by a pervasive Cretaceous thermal disturbance accompanying the emplacement of granitic plutons in the district.

INTRODUCTION

The Fairbanks Mining District

Lode and placer deposits of the Fairbanks mining district define a northeast-trending belt that extends from Ester Dome to Fairbanks Creek and Coffee Dome (figs. 1a, 1b). The mineralized belt is bounded on the northwest by the valley of the Chatanika River. The southeast boundary is approximately parallel to the Chena River valley and its northern tributary.

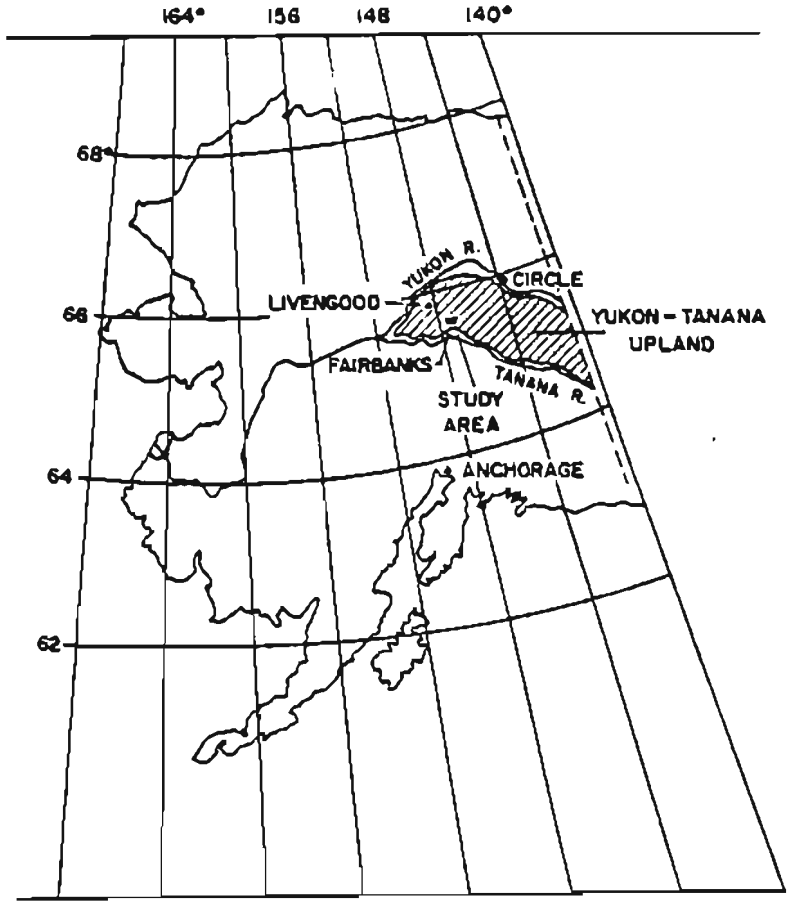

Figure 1a. Map showing location of the Fairbanks mining district.

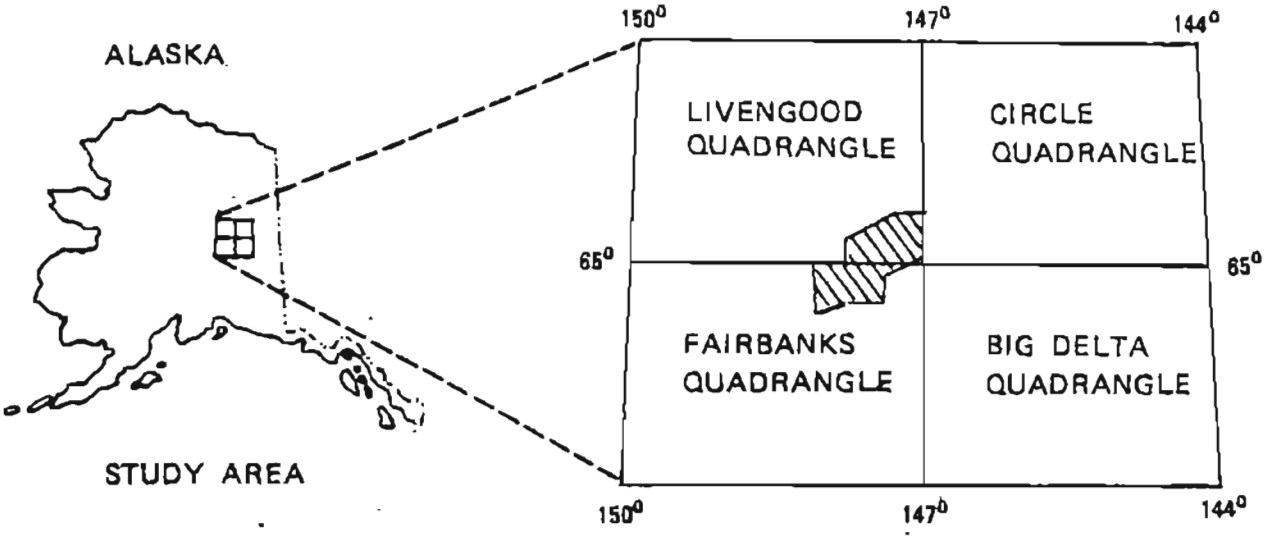

Figure 1b. Location map of the Fairbanks mining district (cross-hatched area); location grid shows the boundaries of the four relevant 1:250,000 U.S. Geological Survey quadrangles.

Mining History

Gold mining and production

The discovery of placer gold in the Fairbanks mining district in 1902 was followed by the onset of widespread placer mining in 1904 that has continued to the present. Nearly $80 million in gold (at $20 per troy oz) was produced by Fairbanks mining district placer-mining operations between 1904 and 1930, before the commencement of large-scale gold-dredging operations. From 1930 to the moratorium on gold mining that was in effect during World War II, placer mining was accelerated by the gold-dredging program initiated by the Fairbanks Exploration Company, and followed to completion by the U.S. Smelting, Refining, and Mining Company in 1964. Smaller placer-mining operations were also active during this period, and the combined gold production has been valued at approximately $130 million.

The first gold-bearing lode was discovered near Chatham Creek in 1903 (Blue Bell claims). According to Hill (1933), it was not until 1908 that much interest was shown in lode prospecting and development. By 1911, however, there were five mills in the district, and 25 to 30 lode properties were under development (Hill, 1933). The high point of early lode-gold mining was reached in 1913, when 12,000 tons of ore were milled in the district. Hill also noted that lode mining was at a 'low ebb' from 1915 to 1923, when the output during any one of these years failed to reach a total of 2,000 tons.

Following the completion of the Alaska Railroad in 1923, lode mining experienced a small revival, and production ranged between 2,700 and 6,000 tons of ore between 1923 and 1930. The larger producers during that period included the Hi-Yu, Mohawk, Rhoads-Hall (Cleary Hill), Wyoming, Tolovana,

Henry Ford, Little Eva, and Eva Quartz Mines (Hill, 1933). A resurgent interest was shown in lode mining during the depression years, and some production was maintained up to the moratorium. Following World War II, however, rising costs and the fixed price of gold prevented the reopening of the lode mines, and until the recent increase in the price of gold, lode activity had been restricted to a few very small scale mining operations and resurgent prospecting and claim improvement.

Hill (1933) estimated that lode mines in the Fairbanks mining district had produced about $2 million prior to 1930, and Berg and Cobb (1967) noted that Fairbanks mining district lodes produced 239,247 oz of gold and 39,078 oz of silver prior to 1960.

Antimony and tungsten production

Antimony and tungsten have also been produced from lode deposits in the district, with small production occurring during various periods when metal prices were favorable. Antimony has been chiefly obtained from stibnite lenses associated with the gold-bearing quartz lodes, and tungsten has been extracted from scheelite associated with skarn deposits adjacent to granitic plutons.

Previous Work

Earliest work on the geology and mineral deposits of the Fairbanks mining district was done by pioneering geologists of the U.S. Geological Survey, including Spurr (1898), Prindle (1905, 1908, 1910a, 1910b, 1913), Prindle and Katz (1909), Chapin (1914), Smith (1913), and Mertie (1918). Following World War I, little published work appeared on the Fairbanks district until Hill's (1933) study of the 'Lode deposits of the Fairbanks district.' Following another quiet period, Byers' (1957) work on tungsten deposits in the Fairbanks district was published as U.S. Geological Survey Bulletin 1024-I.

A preliminary map of the bedrock geology of the Fairbanks mining district (Forbes and Brown, 1961) was followed by the completion of Brown's thesis (1962) on the bedrock geology and ore deposits of the Pedro Dome area.

An accelerated heavy-metals research program involving the combined efforts of the U.S. Geological Survey, U.S. Bureau of Mines, and various private contractors was initiated in 1967; several reports on the bedrock geology and mineral deposits in the district were produced, including Forbes and others, 1968; Chapman and Foster, 1969; Pilkington and others, 1969; Stevens and others, 1969; Britton, 1969; and Hawkins and Forbes, 1971.

Four 1:24,000 quadrangle maps of the geology of the Fairbanks North Star Borough were published by the U.S. Geological Survey in 1975-76 (Péwé and others, 1975, 1976a, 1976b, 1976c).

Other sources of information on the geology and mineral deposits of the district include unpublished B.S. theses by graduates of the University of Alaska School of Mines (College of Earth Sciences and Mineral Industry), and

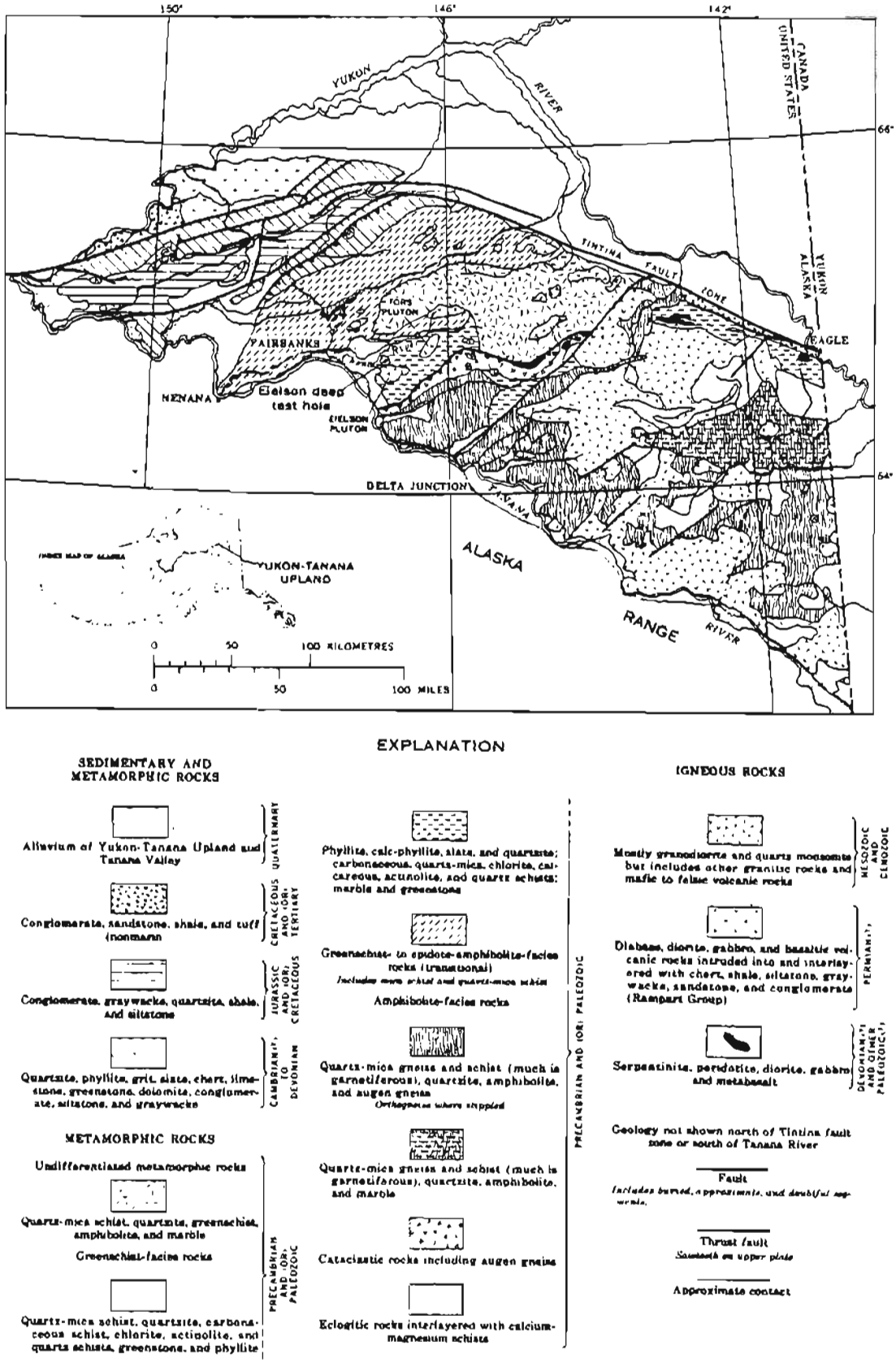

Figure 2. Regional geologic map of the Yukon-Tanana Upland (Forbes and Weber, 1975).

An eclogite-bearing terrane exposed in an apparent structural window north of Fairbanks has yielded a somewhat questionable potassium-argon age of 478.5 ± 35 m.y. (table 1). The structural style is isoclinal-overturned, with northwest-trending fold axes, a trend that is discordant to the northeast-trending fold axes of the schists that compose the upper plate. The northwest-trending folds of the lower plate were subsequently refolded into open synclines and anticlines along the younger northeast-trend (see section on deformational history and structure, p. 50), reinforcing the significance of the apparent 478.5 ± 35 m.y. age of the eclogite-bearing terrane.

Age of the parent rocks

Structural and stratigraphic evidence indicate that greenschist-facies schists in the Circle and Livengood districts include recrystallized late Precambrian and lower Paleozoic sediments (Foster and others, 1973). Poorly preserved Paleozoic fossils have also been found in incompletely recrystallized calc-schists and marbles in the Big Delta and Eagle Quadrangles.

Based on radiometric age data and the above evidence, the metamorphic terranes of the Yukon-Tanana complex appear to have been derived from parental rocks ranging in age from Precambrian to late Paleozoic.

Mesozoic, Sedimentary, and Volcanic Rocks

Sedimentary rocks

Fossiliferous Mesozoic sedimentary rocks have not been found in the southeastern part of the Yukon-Tanana Upland, although a re-entrant of Cretaceous argillaceous sediments, graywackes, and conglomerates has been mapped in the Livengood district, northwest of Fairbanks.

Volcanic rocks

Small areas of tholeiitic basaltic rocks, including pillow basalts, subaerial flows, and breccias occur in the Fairbanks district. These rocks are characteristically preserved in downthrown fault blocks. A preliminary whole-rock potassium-argon age determination indicates that the Birch Hill basalt is of Late Cretaceous age (Kulp and Forbes, unpublished data). However, silicified *Metasequoia* trunks and branches were discovered in a fossil soil zone between the schists and overlying basalts on Birch Hill, which are believed to be of early or middle Tertiary age (Péwé and others, 1976b).

Basalt also occurs as cross-cutting dikes throughout the Upland, and based on compositional similarities to those in the Fairbanks district and on minimal alteration, is probably of Late Cretaceous or early Tertiary age.

Tertiary Sedimentary and Volcanic Rocks

Sedimentary rocks

Tertiary sediments, including siltstones, sandstones, and conglomerates, occur as small, isolated outcrop areas in the Yukon-Tanana Upland. All known

Table 1. Potassium-argon ages of igneous and metamorphic rocks from the Fairbanks mining district, Alaska.

Map number	Sample number	Rock type	Metamorphic terrane	Analyzed sample	Age (m.y.)	References*
1	LK8-9-5	olivine basalt	(not applicable)	whole rock	82.2 ± 3.6	Forbes, Kulp, and Engel (unpublished)
2	Pedro #1	biotite-hornblende quartz diorite	(not applicable)	hornblende	93.0 ± 5.1	Swainbank and Forbes (1975)
3	LK8-10-4	biotite quartz monzonite	(not applicable)	biotite	95.5 ± 2.2	Forbes, Kulp, and Engel (unpublished)
4	LK8-9-1	quartz-epidote-mica schist	Greenschist	white mica	116.4 ± 3.4	" " "
5	LK8-10-8	garnet-quartz-mica schist	Greenschist	muscovite	141.4 ± 2.0	" " "
6	LK8-10-11	quartz-mica schist	Greenschist	biotite	128 ± 4.0	" " "
7	LK8-11-7	garnet-mica schist	Greenschist	whole rock	133.1 ± 4.0	" " "
8	LK8-11-8	quartz-mica schist	Greenschist	muscovite	102.5 ± 3.0	" " "
9	LK8-10-1	garnet-mica gneiss	Amphibolite	muscovite	126.6 ± 3.7	" " "
10	ECDD-12A	amphibolite	Amphibolite	hornblende	245.4 ± 18	Swainbank and Forbes (1975)
11	F49	eclogite	Eclogite	hornblende	478.5 ± 35	" " "
12	F71	pelitic schist	Eclogite	muscovite	117.8 ± 2.6	" " "
13	F136	garnet-hornblende-mica schist	Eclogite	hornblende	135.2 ± 8.0	" " "
14	F136	garnet-hornblende-mica schist	Eclogite	biotite	111.2 ± 3.4	" " "
15	F136	garnet-hornblende-mica schist	Eclogite	white mica	106.1 ± 3.4	" " "
16	LK8-10-9	garnet-mica schist	Eclogite	muscovite	166.2 ± 2.2	Forbes, Kulp, and Engel (unpublished)

*Potassium-argon ages cited from Forbes, Kulp, and Engel (unpublished) were done in the Geochronology Laboratory, Lamont Geological Observatory, Columbia University, by Joan Engels under the direction of J.L. Kulp. Potassium-argon data published by Swainbank and Forbes (1975) were done by Geochron Laboratories, Inc.

occurrences are of continental origin, and some sections contain coal measures and/or basal basalts. The lithology and stratigraphy of these sections are similar to those of the coal-bearing Tertiary sections on the north flank of the Alaska Range.

Volcanic rocks

A large Tertiary volcanic field dominated by felsic volcanic rocks, including welded tuffs, has been mapped in the Tanacross Quadrangle by Foster (1970). The volcanic suite is similar to that of the Tertiary volcanic fields of the Great Basin or the Circum-Pacific island arcs. Possible caldera structures have also been described by Foster (1970).

Although this field was much more extensive in Tertiary time, it is now preserved as erosional remnants at higher elevations in the Upland. Dacite flow units belonging to this sequence are cut by the Cathedral Bluffs fault on Sixtymile Butte, north of Tok Junction (Foster, 1970).

Quaternary Volcanism and Surficial Deposits

Volcanic rocks

Quaternary basalts are present in several areas in the Tanacross Quadrangle. Prindle Volcano, located about 45 mi northeast of Tetlin Junction, is a small alkali-basalt cone that rests on granodiorite basement. The breached cone is associated with a small lava flow that moved down the east slope of the cone and turned southwest down the valley of the east fork of Fortymile River. The basalts of Prindle Volcano contain exotic fragments of deep crustal and mantle rocks (Foster and others, 1966).

A small outcrop of Quaternary basalt is located at the old CANOL pump station southeast of the Tanacross airstrip, and several more occurrences have been mapped adjacent to northeast-trending faults in the Upland within the Tanacross Quadrangle. The tectonic significance of faults and basalt eruptive centers is discussed below.

Glacial history

Although fragmentary evidence suggests that glaciation in interior Alaska may have been initiated in late Miocene or Pliocene time, moraines and outwash of the Delta (inferred early Wisconsinan) Glaciation mark the onset of major late Pleistocene glaciation in the northeastern part of the Alaska Range (Péwé and Holmes, 1964; Holmes and Foster, 1968; Weber and others, 1981). The Delta Glaciation, following the Sangamon Interglaciation, was followed by the Donnelly (late Wisconsinan) Glaciation.

Both Illinoian and Wisconsin glaciations have left a record in the northeastern Alaska Range and the Yukon-Tanana Upland. Glaciation in the Upland was restricted to local alpine glaciation systems that developed in the higher hills and included relatively small distributary valley glaciers. However, valley glaciers descending the north slope of the Alaska Range reached the flood plains of the Tanana, Delta, and Tok Rivers, as documented

by moraines and glaciofluvial deposits that have been identified and mapped by Péwé and Holmes (1964) and others.

Glacial advances were accompanied by a great increase in the amount of suspended sediment carried into the master streams by tributaries descending the north slope of the Alaska Range. As a result, the Tanana, Delta, and Tok Rivers aggraded their channels, causing lateral migration and meandering across the valley floor at a rate that was too rapid for the development of vegetation on the valley floor. Therefore, southerly winds were able to pick up large quantities of silt from the flood plains and deposit it in the Upland to the north, as 'loess.'

Alluvial and colluvial deposits

During Holocene time (<10,000 yr B.P.), tributary streams in the Upland initiated a new cycle of downcutting. Master streams are no longer overladen with glacial debris, and geodetic measurements indicate that the Tanana valley is subsiding and that the Alaska Range is undergoing relative uplift. Under these conditions, glacial deposits are being reworked by master streams in the flood plains, and colluvial deposits are developing in the Upland.

Permafrost

During Wisconsinan time, the 0°C isotherm may have reached depths of 1,200 ft in the Yukon-Tanana region. During the last 2,000 or 3,000 yr, a warming trend has initiated a long-term thawing cycle. Currently, the permafrost table is deepest on north-facing slopes, and valley floor alluvial fill is covered by vegetation. Broad valleys, floored by flood-plain deposits, are underlain by discontinuous permafrost. South-facing slopes are generally free of permafrost.

Regional Tectonic History

Tectonic framework

The regional tectonic setting is dominated by the Tintina and Denali faults (fig. 3). Both of these strike-slip faults have experienced large-scale right-lateral displacement, bringing crustal blocks of contrasting geology into contact along the trace of the faults. Roddick (1967) estimated that there may have been 40 mi (64 km) of right-lateral offset along the Tintina lineament in Paleozoic time, with an additional 220 mi (675 km) of offset during the Mesozoic Era. Right-lateral slip along the Tintina fault seems to have decreased markedly during early Tertiary time in favor of strain release along the Denali fault system. Forbes and others (1976) cite geologic evidence to support a right-lateral offset of 250 mi (725 km) along the Denali fault since Late Cretaceous time, a displacement that gives an average slip rate of 0.62 cm/yr during the previous 65 m.y.

Although the Tintina fault appears to be locked, the Denali fault is active between Denali National Monument and the juncture with the Totschunda fault (Forbes and others, 1976). Based on the recent findings of Plafker and others (1978), some of the strain that was formerly released along the Denali

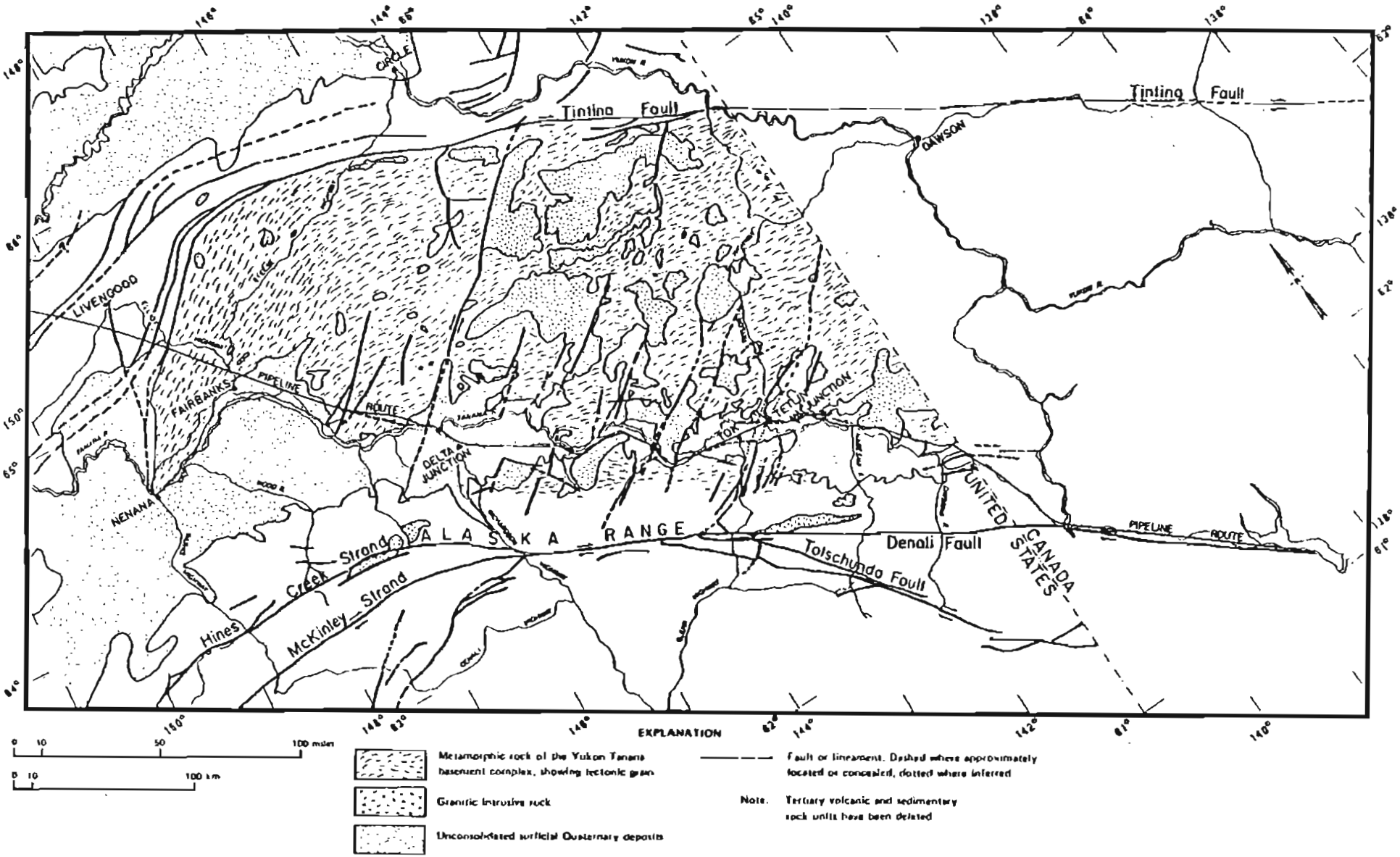

Figure 3. Tectonic map of the Yukon-Tanana Upland (compiled by Forbes, 1980).

fault is now released by slip along the Totschunda and Fairweather faults. The record seems to indicate the successive development of regional strike-slip faults toward the continental margin, with changing subduction rates and flow vectors of the Pacific plate. Plafker and others (1978) have measured offsets of Holocene glacial deposits and geomorphic features along the trace of the Fairweather fault that indicate an average right-lateral displacement rate of 5.8 cm/yr over the last millenium. Such a rapid displacement rate suggests that the Fairweather fault is acting as a transform plate boundary, and that the Denali fault may be a former transform fault that is now being bypassed by the Fairweather fault. Seismic activity indicates that considerable strain release is still occurring along the Denali fault, but it is clear from comparative Holocene displacement rates and major earthquake activity over the last 100 yr that the Fairweather is the successor transform system.

Tectonics of the Yukon-Tanana crystalline block

As defined above, the Yukon-Tanana block is bounded on the northeast and southwest, respectively, by the Tintina and Denali faults. The oldest structural grain in the block trends to the northwest, but a superimposed northeast trend becomes increasingly dominant in the northwestern part of the block. The northeast-trending folds transect the older grain at an angle of approximately 60°. The later deformational episode occurred about 90 to 120 m.y. B.P., and was associated with the emplacement of ore deposits and the younger generation of granite plutons.

Potassium-argon age data obtained from core from a 9,800-ft-deep test hole near Eielson Air Force Base (fig. 2), indicate that amphiboles in the basement complex passed through the argon-blocking isograd about 180 m.y. B.P. (D.L. Turner and R.B. Forbes, unpublished data). Using a calculated fossil geothermal gradient of 33°C/km and an argon-blocking temperature of 350°C, approximately 11 km of overlying crust have been removed by erosion during the last 180 m.y., an uplift rate of 0.05 mm/yr. Although granulite-facies inclusions were brought up from the deep crust by the alkali basalts of Prindle Volcano (fig. 2; Foster and others, 1966), metamorphic rocks of such high grade are not known to exist in outcrop in the Upland. It is clear that erosion hasn't yet exposed the deep roots of the complex, and that uplift has proceeded at a relatively slow rate since Mesozoic time.

We do not have the necessary geodetic measurements to know whether or not the Upland north of the Tanana River is presently undergoing relative uplift. However, level-line surveys conducted by the Coast and Geodetic Survey before the Good Friday Earthquake indicate that the Tanana valley is subsiding, while the Alaska Range is continuing a cycle of relative uplift that dates to Pliocene time.

Recent geologic mapping (Foster, 1970; Weber and others, 1977) and aeromagnetic studies (Griscom, 1976) show that the Yukon-Tanana block is transected by several northeast-trending fault systems that can be traced across the Tanana valley into the highlands to the south, where they are truncated by the Denali fault. Several of these, including the Shaw and Mansfield Creek faults, show left-lateral offsets and appear to be large-scale dislocations related to a possible shear couple between a locked or relatively

slow moving Tintina fault and more active displacement along the Denali fault system (fig. 3).

Perhaps the lack of recognizable Holocene offset and historically documented earthquake-related strain release along most of these faults can be used as indirect evidence for decreasing displacement rates along the Denali fault. It should be noted here, however, that earthquake hypocenters in the Fairbanks mining district are part of a northeast-trending zone of earthquake activity that extends from the Alaska Range beyond Fairbanks into the Yukon basin. To date, this earthquake belt has not been correlated with fault systems exposed on the surface in the Fairbanks mining district.

PETROLOGY OF THE METAMORPHIC ROCKS

Regional Metamorphic Setting

In summarizing the lithology of the 'Birch Creek Schist Formation,' Mertie (1937) stated that it consisted principally of quartzite, quartzite schist, quartz-mica schist, mica schist, feldspathic and chloritic schists, and a minor proportion of a carbonaceous and calcareous schist and crystalline limestone (marble). He further stated that micaceous quartzites and quartz-mica schists were the most common rock types. Continuing work has shown, however, that the Birch Creek (Yukon-Tanana complex) terrane also includes a wide variety of gneisses, calc-magnesian schists, and phyllites. Mineral assemblages composing the metamorphic rock types of the Yukon-Tanana Upland range from greenschist to eclogite facies, but the areal distribution of metamorphic facies and subfacies within the Birch Creek terrane is still not well understood due to insufficient data and complex petrologic relations.

Two belts of low-grade (greenschist-facies) rocks were differentiated in the Birch Creek Schist Formation by Mertie (1937) as a pre-Middle Ordovician sequence. One belt extends from the Tatalina River northeastward approximately 90 mi to the north fork of Preacher Creek; a second belt can be traced from the lower Chena River valley eastward into the Fortymile district, where it is cut by the intrusive granitic rocks of the Charley River batholith.

Rock types grouped by Mertie under his pre-Middle Ordovician map unit include slates, argillites, limestone, feldspathic arkose, graywacke, quartzite, phyllite, and greenstone. Some of these rock units were mapped by earlier workers as the Tatalina Group (Prindle, 1913), and they were believed to be of Ordovician age. Mertie (1937) listed an Early Ordovician faunal assemblage collected by E. Blackwelder in 1915 from slates and argillites on the southeast fork of Willow Creek, in the White Mountains, as supporting evidence for a pre-Middle Ordovician age.

There is little correlation between the two pre-Middle Ordovician belts in respect to lithology and structural setting, and there does not appear to be any further justification for maintaining 'pre-Middle Ordovician sequence' as a formal stratigraphic term. Greenschist-facies rocks comprise a mappable unit, however, and this appears to be a more rational approach to the problem.

The petrology and tectonic setting of the low-grade metamorphic rocks in each of these belts must be further investigated if the complex petrogenesis of the crystalline terranes is to be understood. It is possible that the greenschist-facies rocks of the Chena-Fortymile belt may define a younger sequence of crystalline schists than is represented by the higher grade rocks occurring to the north and south, or that the two terranes are in fault contact along a thrust surface that was folded during Late Cretaceous and (or) early Tertiary time.

Range in Metamorphic Facies and Lithology

The metamorphic rocks of the Fairbanks district were first classified as 'Birch Creek Schist,' as correlated with the type locality at the head of Birch Creek, a few miles south of Circle, Alaska (Spurr, 1898). Buff- to brown-colored quartz-mica schists and micaceous quartzites of the greenschist facies are exposed at the type locality. Although similar rock types occur in the Fairbanks mining district, other rock types, including those of higher metamorphic facies, are also present. As discussed in the preceding section, the formational term 'Birch Creek Schist' has been rejected in favor of Yukon-Tanana crystalline complex, as applied to the metamorphic rocks underlying the Yukon-Tanana Upland.

Distribution of Facies and Rock Types

Based on structural and petrologic constraints, the metamorphic rocks of the district can be grouped into three packages:

- Greenschist facies: Quartz-mica (± garnet) schists and micaceous quartzites, with subordinate greenschist, calc-mica schists, thin layers of marble, calc-phyllites, and quartzites, with very little mica and slate.

- Garnet-amphibolite facies: Amphibolites, gneisses, garnet-mica schists, plagioclase-epidote-mica schists, and marble.

- Eclogite facies: Eclogites, calc-eclogites, diopside marbles, garnet-mica schists, and graphitic quartzites.

The eclogite-facies suite is restricted to what appears to be a tectonic 'window' on the northwest flank of the divide between the Chatanika River valley and Pedro and Cleary Creeks. The garnet-amphibolite-facies rocks occur along the axial trace of a synform that can be traced from roadcrops near the intersection of Sheep Creek and Goldstream Roads, to Fox and northeast to the ridge between Solo and Fish Creeks. Outcrops of these rocks have also been mapped on the higher elevations of Chena Ridge. The greenschist-facies suite is widely distributed on the higher ridges in the district and adjacent areas, where the outcrops are usually characterized by blocky, dark-brown-colored micaceous quartzites and quartz-mica schists. Slightly lower grade calc-phyllites, quartzite, and slate occur on the southern margin of the area. Structural and radiometric age data suggest that this latter group of rocks is a younger metamorphic sequence or terrane that structurally overlies the other

terranes. However, the interrelationship between the eclogite- and amphibolite-facies terranes is not clear.

Greenschist-facies Suite

Micaceous quartzites and quartz-mica schists

These rocks have a relatively simple mineralogy and grade into feldspathic quartz-mica schists with a modal increase in plagioclase feldspar (albite) exceeding 10 volume percent. A similar transition into pelitic schists is accomplished with the appearance of garnet and a relative modal increase in muscovite and/or biotite. Representative mineral assemblages are:

- Quartz-muscovite-albite (± chlorite)
- Quartz-muscovite-albite-biotite (± garnet, chlorite)

Accessory minerals include apatite, zircon, tourmaline, magnetite, potassium-feldspar, and various sulfides. At some localities, the feldspathic quartz-mica schists contain minor rather than trace concentrations of sulfides and are of interest as possible economic targets.

Pelitic schists

Volumetrically, pelitic schists are subordinate to the other metasediments in the greenschist-facies terrane, based on the original definition that implies a clay-rich protolith. Pelitic compositions are characterized by muscovite approaching 50 percent and the appearance of garnet grains that are usually less than 0.3 mm in diameter. Biotite is less abundant than muscovite, and seldom accounts for more than 10 percent of the rock. Chlorite is ubiquitous and appears to be in metastable equilibrium with incipient biotite in some assemblages. Characteristically, the alumina-excess minerals (staurolite, andalusite, kyanite, and sillimanite) have not been found in rocks of the greenschist-facies terrane, with the exception of hornfelsed pelitic schists that have been upgraded by thermal metamorphism adjacent to granitic plutons. A representative pelitic mineral assemblage is documented in table 2. Accessory minerals are similar to those described for the feldspathic schists, with a relative increase in trace tourmaline and zircon.

Feldspathic quartz-mica schists

These rocks are transitional with both pelitic and quartz-mica schists, and may contain small amounts of potassium feldspar in addition to sodic plagioclase. A typical mineral assemblage is listed in table 2.

Calc-magnesian schists

Calc-magnesian schists are relatively rare in the greenschist-facies terrane. Variants include greenschists and phlogopite-chlorite-epidote-albite and quartz-carbonate-phlogopite schists. Typical mineral assemblages are listed in table 2. Accessory minerals in the calc-magnesian schists include sphene (leucoxene), apatite, magnetite, and rare zircon.

Table 2. Approximate modes of representative rock types from the greenschist-facies terrane, Fairbanks mining district, Alaska (modified from Brown, 1962).

Rock type	Quartz (%)	Albite (%)	Muscovite (talc*) (%)	Chlorite (%)	Biotite (phlogopite*) (%)	Garnet (%)	Potassium-feldspar (%)	Actinolite (tremolite*) (%)	Epidote (%)	Carbonate (%)	Carbonaceous material (%)	Accessories (%)
Micaceous quartzite	77	71	2	14								1
Quartz-muscovite schist	21	5	56	15	trace						3	
Feldspathic quartz-mica schist	36	25	30	3	5	trace						1
Pelitic (garnet-mica) schist	20	10	46	5		15						4
Greenschist		20		6				65	9			
Phlogopite-albite-chlorite schist		27		45	20*				3	5		
Tremolite-talc		2	7*		3			5*		83		

Marbles

Marbles are the rarest of all rock types in this terrane and are usually associated with the above calc-magnesian schists, as relatively thin (1-m-thick) units. Mineral assemblages include:

- .Carbonate-tremolite-talc-quartz
- .Carbonate-quartz

Accessories include apatite and carbonaceous material. Table 2 lists representative modes for the above rock types.

Quartzite and slate

Found only on Birch Hill, these lower greenschist-facies rocks (metasiltstone, quartzite, and slate) have a typical mineral assemblage of quartz-albite-sericite. Garnet is totally absent.

Amphibolite-facies Suite

The amphibolite-facies suite includes the following rock types:

- .Micaceous quartzites and quartz-mica schists
- .Garnet-mica (pelitic) schists
- .Gneisses
- .Ortho-amphibolites
- .Para-amphibolites
- .Calc-magnesian schists
- .Marbles

Micaceous quartzites and quartz-mica schists

The mineralogy of these rocks is similar to that of the same rock types that occur in the greenschist-facies terrane. Although the average grain size is larger, the appearance in outcrop is also similar to the quartzites and quartz-mica schists that occur in the greenschist-facies terrane.

Garnet-mica (pelitic) schists

These schists are conspicuously more coarse grained than rocks with a similar mineralogy that are also present in the greenschist-facies terrane. The most typical mineral assemblages are:

- .Quartz-plagioclase-muscovite-garnet
- .Quartz-plagioclase-muscovite-biotite-garnet

Gneisses

Gneissic rocks are among the rarest in the district and appear to be associated with the amphibolite-facies terrane. Two known variants are a medium-grained, porphyroblastic variant in the headwaters of Pedro Creek and the divide between Solo and Bear Creeks and an extremely coarse-grained flaser

gneiss that crops out at the base of the bluff just west of the old Fox Roadhouse. The mineralogy of both types of gneiss is similar, as documented by the mineral assemblages in table 3.

Table 3. Representative modes of gneissic rocks from the Fairbanks mining district, Alaska (from Brown, 1962).

Mineral	Sample number and percent by volume 37-6 (%)	50-1 (%)	79-1 (%)	79-2 (%)	82 (%)
Potassium feldspar	12	20	40	25	25
Plagioclase feldspar	17	30	25	20	25
Quartz	46	15	20	30	15
Biotite	6	6	7	10	5
Muscovite	9	15	5	5	4
Epidote	9	10	-	3	15
Calcite	a	-	-	-	-
Orthite	a	a	-	a	a
Sphene	a	-	-	-	a
Apatite	-	a	a	a	-
Rutile	-	-	a	a	a
Pennine	a	3	2	5	10
Magnetite	-	-	-	1	-
Zircon	a	-	a	a	-

a = accessory mineral, less than 1 percent

The plagioclase is usually oligoclase, and epidote, chlorite, apatite, rutile, orthite, magnetite, and sphene are common accessories. Representative modes of the gneissic rocks are shown in table 3. Potassium-feldspar is very rare as a mineral phase in Fairbanks district metamorphic rocks, and these gneisses are the only known metamorphic rock type in the district to contain potassium feldspar as a major mineral phase. The gneisses are pervasively retrograded and show evidence of late cataclasis that is probably related to a second and later deformational event.

Ortho-amphibolites

These rocks, which consist of over 50 percent hornblende, are quite homogeneous and contain a well-defined crystallization foliation and 'b' lineation defined by the preferred orientation of hornblende. A chemical analysis of an ortho-amphibolite from the marble quarry near Fox is shown as F229 in table 4. Inspection of the analysis shows that the whole-rock composition is analogous to that of a tholeiitic basalt of the 'continental' or island-arc type. During earlier work, garnet was not found in any of the ortho-amphibolite assemblages, and because of this, the facies assignment was thought to be that of the lower amphibolite (epidote-amphibolite) facies. Unfortunately, the facies assignment is complicated by the appearance of garnet in aluminous layers in para-amphibolites derived from tuffaceous sediments. However, due to the absence of diopsidic pyroxene in the amphibolites and calc-magnesian schists, and the lack of kyanite and/or

Table 4. Whole-rock chemical analyses and CIPW norms of metamorphic rocks from the eclogite-facies terrane, Fairbanks mining district, Alaska.

	Pelitic schists				Amphibolites				Eclogitic rocks					
	Qz-Ar-Musc-Chlor		Gt-Qz-Musc-Ab		Am	Gt-Am-Gt-Qz			Gt-Px-Am-Gt-Qz			Gt-Px-Gt-Qz		
Oxide	F10	F11	F29	F71	F229[a]	F230[a]	F136	F162	F50	F86	F89	F39	F101	F201
SiO_2	55.03	60.64	53.87	62.79	51.06	41.99	42.95	47.21	35.22	68.26	38.90	28.61	30.02	54.61
TiO_2	0.75	1.39	3.96	1.26	1.19	3.03	1.31	0.73	2.71	0.88	2.32	2.63	2.45	1.69
Al_2O_3	24.51	15.81	17.49	15.48	14.54	20.46	14.52	12.01	9.34	10.01	6.46	9.71	8.58	12.92
Fe_2O_3	4.77	1.90	3.80	1.80	2.58	2.49	2.34	2.47	3.14	4.06	5.07	3.58	3.41	3.91
FeO	1.24	7.42	1.16	4.97	8.81	14.01	6.90	8.58	5.89	5.41	5.85	10.15	10.11	4.97
MnO	0.03	0.09	0.02	0.11	0.15	0.14	0.14	0.32	0.13	0.17	0.44	0.42	0.66	0.14
MgO	1.50	4.02	3.38	2.56	6.15	5.38	7.49	13.68	9.66	3.66	7.39	6.80	4.63	6.51
CaO	0.13	1.56	3.20	1.77	9.69	5.92	10.85	10.57	19.73	5.43	23.22	22.32	24.00	11.79
Na_2O	0.79	1.32	1.78	1.56	3.84	3.23	1.53	1.49	0.63	1.63	1.59	1.52	2.22	1.51
K_2O	6.37	2.87	4.03	4.42	0.43	1.08	3.17	0.20	1.39	0.13	0.04	0.09	0.07	0.24
P_2O_5	0.07	0.09	0.32	0.09	0.12	0.07	0.17	0.18	0.25	0.04	2.09	3.09	2.02	0.21
H_2O+	5.01	2.47	6.17	2.91	1.56	2.11	1.84	2.70	6.64	0.59	1.04	7.03	3.24	1.73
H_2O-	0.13	0.15	0.10	0.05	0.18	0.11	0.10	0.13	0.05	0.05	0.00	0.05	0.10	0.00
Cr_2O_3	0.0072	0.012	0.054	0.0052	n.d.	n.d.	0.042	0.046	0.023	0.018	0.0039	0.0031	0.0091	0.072
NiO	0.0036	0.0066	0.0026	0.0028	n.d.	n.d.	0.0018	0.0072	0.0008	0.0049	0.0005	0.0058	0.0029	0.0075
CO_2	n.d.	n.d.	n.d.	n.d.	n.d.	n.d.	6.62	n.d.	5.42	0.08	6.22	4.16	8.24	n.d.
Total	100.34	99.75	99.84	99.78	100.30	100.02	99.97	100.36	100.22	100.42	100.63	100.17	99.76	100.31
S.G.	2.826	2.808	2.892	3.100	3.033	3.158	n.d.	n.d.	3.163	3.003	3.010	3.420	3.355	3.255
Quartz	23.45	27.82	17.23	26.29	- -	- -	11.07	- -	- -	39.15	0.08	- -	- -	14.76
Orthoclase	40.14	17.95	25.90	27.63	2.58	6.61	17.10	1.20	8.20	0.80	0.24	0.54	0.47	1.47
Albite	7.57	12.55	17.38	14.82	35.06	25.89	12.55	13.59	5.65	15.33	14.61	10.64	8.93	14.06
Anorthite	0.20	7.57	14.99	8.67	21.52	29.97	7.73	25.90	18.54	20.54	10.61	19.85	13.49	28.80
Nepheline	- -	- -	- -	- -	- -	2.50	- -	- -	- -	- -	- -	1.99	6.83	- -
Corundum	18.92	9.14	6.71	5.92	- -	3.82	5.45	- -	- -	- -	- -	- -	- -	- -
Diopside	- -	- -	- -	- -	21.25	- -	- -	20.95	11.57	5.92	43.59	11.65	23.98	24.35
Hypersthene	4.42	20.61	10.15	12.62	7.82	- -	25.66	19.76	20.09	12.42	2.14	- -	- -	9.35
Olivine	- -	- -	- -	- -	7.06	23.96	- -	14.50	3.09	- -	- -	17.87	9.18	- -
Magnetite	1.48	2.11	- -	1.99	2.74	2.69	2.27	2.68	3.30	4.47	5.42	3.83	3.63	4.32
Ilmenite	1.11	2.05	1.99	1.86	1.68	4.37	1.67	1.03	3.77	1.28	3.31	3.75	3.48	2.44
Apatite	0.16	0.20	0.73	0.20	0.25	0.15	0.32	0.38	0.52	0.09	4.47	6.61	4.30	0.46
Calcite	- -	- -	- -	- -	- -	- -	16.17	- -	25.26	- -	15.53	23.27	25.77	- -
Hematite	2.56	- -	2.92	- -	- -	- -	- -	- -	- -	- -	- -	- -	- -	- -
Rutile	- -	- -	2.01	- -	- -	- -	- -	- -	- -	- -	- -	- -	- -	- -

[a]Analyses: H. Matsumoto and H. Haramura
All other analyses: H. Haramura and T. Katsura

staurolite in adjacent pelitic schists, assignment of this sequence of rocks to the lower amphibolite facies is probably merited. The characteristic mineral assemblage is:

.Hornblende-plagioclase (± epidote, biotite, quartz)

Sphene is a ubiquitous accessory, along with apatite and rutile. Rutile, when present, is usually surrounded by jackets of sphene.

Para-amphibolites

Superficially these amphibolites appear to be similar to the ortho-amphibolites in outcrop, but closer examination shows that they often contain lenses of carbonate and metasedimentary layers. Microscopically these amphibolites often contain quartz, carbonate, epidote, garnet, and biotite as minor constituents. The most characteristic mineral assemblage is:

.Hornblende-plagioclase-quartz (± garnet, carbonate, epidote, biotite)

Some amphibolites contain major carbonate and are classified as calc-amphibolites. Plagioclase is usually in the oligoclase compositional range. Accessory minerals include sphene, rutile, apatite, magnetite, and zircon.

Calc-magnesian schists

Rocks assigned to this category include those rocks other than amphibolites and marbles that are dominated by calcium and/or magnesium-rich mineral phases. Definitive mineral assemblages include:

.Quartz-amphibolite-epidote
.Carbonate-amphibole-epidote
.Amphibole-garnet-biotite-quartz

Accessory mineral phases include sphene, apatite, epidote, magnetite, and rare zircon.

Marbles

Marbles associated with the amphibolite-facies terrane are relatively pure carbonate rocks ranging in thickness from a few inches to 40-50 ft at the Fox quarry. The marbles are closely associated with amphibolites at Fox and in the roadcrops near the junction of Sheep Creek and Coldstream Roads, northeast of Ester Dome. Accessory minerals include tremolite, epidote, and opaques.

Eclogite-facies Terrane
(modified from Swainbank and Forbes, 1975)

As mentioned in the introduction, the eclogite-bearing terrane appears to be a tectonic window, or fault block. Structural and geochronological

evidence for this conclusion are discussed in more detail in following sections.

Quartzites, micaceous quartzites, pelitic schists, eclogites, amphibolites, and impure marbles have been mapped and studied in the eclogite-bearing terrane. A brief petrographic description of these rock types follows.

Quartzites and micaceous quartzites

These rocks are present in both the upper and lower (eclogite-bearing) sequences and are the dominant units in the upper plate. The essential mineralogy is quartz, muscovite, biotite, garnet, and chlorite. Accessories include apatite, magnetite, zircon, and tourmaline.

Although these rocks are of similar appearance in outcrop in both sequences, chlorite appears to be a stable essential phase in the upper-sequence assemblages, but it is a retrograde mineral in the lower plate.

Quartzites in the eclogite-bearing part of the lower sequence are often rich in carbon and dull black in outcrop. Parent rocks appear to have been siliceous siltstones with a high content of organic carbon.

Pelitic schists

The typical mineralogy is quartz-garnet-muscovite-plagioclase (± biotite, chlorite). Rutile, sphene, apatite, and opaques are frequent accessories. The quartz fabric is usually granoblastic, and the untwinned plagioclase occurs as albite-oligoclase porphyroblasts.

Subhedral muscovite shows a strong preferred orientation, and skeletal garnet porphyroblasts enclose subparallel laths of muscovite and biotite. Biotite occurs as a major constituent in a few variants and as a minor or trace component in most pelitic schists. Chlorite (pennine) is faintly pleochroic in green and olivine green and is present in the eclogite-bearing terrane only in retrograded rocks.

Kyanite and staurolite (relict) were found in one pelitic schist collected near the old Cleary Village site by J.M. Brown (1962). Subsequent work by Swainbank and Forbes (1975) in the eclogite-bearing terrane failed to produce kyanite-bearing pelitic schists at other localities.

Impure marbles

Some of the rocks composed of the assemblage carbonate-clinopyroxene-garnet (± amphibole, phlogopite, epidote) contain more than 50 percent carbonate, and according to most classification systems should be termed marbles (lime-silicate marbles). Such rocks are intercalated with carbonate-bearing eclogitic rocks and calc-amphibolites.

Eclogites and garnet amphibolites

Three calc-magnesian variants occur in the eclogite-facies terrane that correspond to types 'a,' 'b,' and 'c' as described by Prindle (1913): (1)

garnet-clinopyroxene (± calcite, quartz, plagioclase, epidote); (2) garnet-clinopyroxene-amphibole (± calcite, quartz, plagioclase, epidote); and (3) garnet-amphibole (± calcite, quartz, plagioclase, epidote).

Muscovite or phengite achieves major modal proportions in some variants, and apatite, sphene, and opaques are frequent accessories. Biotite, secondary chlorite, rutile, and abundant carbonaceous material are also frequent accessories in type (3) rocks.

Garnet-Clinopyroxene Rocks (Eclogites)

Fabrics vary from mylonitic, layered, and/or laminated varieties to massive types. Pale-pink garnets are usually poikiloblastic. Garnets contain abundant clinozoisite, calcite, and quartz inclusions. Garnet grains often display rims of blue-green amphibole as a reaction product (kelphytic rims).

Fresh, pale-green, omphacitic pyroxene greatly predominates over the highly altered, dark-green, diopsidic pyroxene that is also present in some variants.

Untwinned albite is present only in the mylonitic variants and is usually associated with garnet, clinopyroxene, and chlorite. Quartz generally occurs as granoblastic aggregates, and calcite occurs as an essential phase along with clinopyroxene and garnet. Carbonate also occurs as discordant veinlets that cut the earlier foliation.

Pseudomorphic aggregates of epidote and quartz after garnet are occasionally present, but clinozoisite is present as a more abundant and stable phase that attains major component proportions in certain compositional layers in some eclogitic rocks.

Sphene is the dominant titanium-bearing phase, and apatite, orthite, and opaques are common accessories.

Garnet-Clinopyroxene-Amphibole Rocks

Fabric variations are more limited than those described for the preceding group, and finely laminated and massive varieties are dominant. Garnets are typically helicitic and are characterized by euhedral overgrowths on subhedral poikiloblastic cores. Inclusion trains include clinozoisite, quartz, and calcite.

The clinopyroxene, which is pleochroic to light green, is usually poikiloblastic. The amphibole is pleochroic in pale green with little absorption and grades to a dark-green and more highly absorptive hornblende next to garnet grains.

Plagioclase (albite-oligoclase) is more abundant than in the amphibole-free variants, and tends to occur in the stress shadow areas adjacent to garnets and clinopyroxene porphyroblasts. Muscovite is often present and is present in both the earlier synkinematic fabric and in transecting shear planes.

Calcite is more abundant than quartz, and no reaction has been observed between the two phases. Discordant veinlets of both minerals cut the foliation.

Clinozoisite is the most common of the epidote-group minerals, but zoisite is also present in the more siliceous variants. Both minerals are frequent inclusions in the garnet porphyroblasts.

Apatite occurs as aggregates and as individual grains, and sphene occurs both as rims armoring rutile and as discrete grains of aggregates. Tourmaline, orthite, and graphite are also present as accessory minerals.

Garnet-Amphibole Rocks

Fabrics vary from rather massive types to those with an incipient foliation. Garnet porphyroblasts are large (up to 8 mm diameter), with euhedral overgrowths on subhedral poikiloblastic cores. Helicitic garnets are rare, and many grains have kelyphitic margins.

Rocks containing synkinematic, subhedral amphibole grains (X = pale green; Y = green; Z = deep green) are the most ubiquitous, but some rocks contain an amphibole with another distinctive pleochroic scheme (X = colorless; Y = green; Z = green blue).

Untwinned plagioclase grains are common, and complex plagioclase porphyroblasts were observed in several specimens.

Muscovite and biotite are initial synkinematic phases in many of these rocks, but late muscovite is also present along discordant S_2 planes. Late biotite grains that are discordant to the foliation are also present. Clinozoisite is a major mineral phase in some compositional layers. Sphene, rutile, apatite, and opaques are accessories. Rutile is the dominant titanium-bearing phase. Carbonaceous material, though not modally important, is much more abundant in this group.

Whole-rock analyses of rocks from the eclogite-facies terrane

In order to minimize possible geographic variation in the P/T conditions accompanying recrystallization, most of the analyzed rocks were collected by Swainbank and Forbes (1975) from one locality (a borrow pit at 6.1 Mi Elliott Highway). However, two garnet-mica schists (F10-F11, table 4) and one amphibolite (F162, table 4) were collected from adjacent localities. Bulk chemical, modal, and CIPW norm data for these rocks are presented in tables 4 and 5.

Comparative Chemical and Normative Composition of the Eclogitic Rocks

An examination of these analyses and their respective norms (table 4) and modes (table 5) shows that although the undersaturated variants have normative nepheline, olivine, and calcite, only calcite appears in the mode. Orthopyroxene was not detected in any of these assemblages, although hypersthene appears in four of the norms.

All eclogitic variants are anorthite normative, but calcic plagioclase does not appear in the mode, although minor amounts of albite were detected in some of the analyzed eclogitic rocks.

Some of the normative anorthite is expressed in the mode as clinozoisite, but most of the normative anorthite is present in the garnet as the grossularite component.

Sedimentary vs Mafic Igneous Analogs

The compositional field as defined by FMA-CNK plots of the analyzed eclogitic rocks (fig. 4) does not coincide with the field defined by plots of 'C' - type eclogites (eclogites associated with blueschist) (Coleman and others, 1965). The high MgO/FeO ratio displaces the Fairbanks calc-eclogites from the tholeiite trend, and the alkali-olivine basalt trend is completely dissimilar. No correlation can be made between the eclogites of the Fairbanks mining district and the usual compositional trend for basic igneous rocks, as seen on the ACF diagram (fig. 5), where the Fairbanks eclogites are compared with compositional fields of ultramafic and mafic igneous rocks and analyzed eclogites reported in the literature.

Proposed Sedimentary Parentage

As shown in figure 6, most of the eclogites from this study fall outside the compositional field of typical eclogites, indicating that the layered, carbonate-bearing eclogites represent a newly recognized compositional variant among the eclogitic rocks. Furthermore, many of the calc-eclogites have chemical compositions that are compatible with basaltic or basic igneous rocks.

Many of the carbonate-free eclogites and garnet amphibolites of the Fairbanks mining district are also distinguished from rocks of typical basaltic composition by their low Na_2O/K_2O ratios (F136, table 4) or by their high SiO_2 content.

The analyzed rocks are compared in the ACF diagram (fig. 6) with a selection of representative sedimentary rocks. It is evident that the carbonate-bearing eclogites are compositionally analogous to marls and that the less calcareous variants are comparable to subgraywackes.

Hahn-Weinheimer (1960) and Smulikowski (1964, 1965) have reported eclogites of probable sedimentary origin. The chemical similarity of the carbonate-bearing eclogites of the Fairbanks area to known sedimentary rocks and the concordant relationships of the eclogitic rock units within the sequence lead us to conclude that the calcareous variants are of metasedimentary parentage.

According to F. Frey (1971, written commun.), 'In further support of the probable sedimentary origin of these eclogitic rocks, the rare-earth elements in a calcareous eclogite from Cleary Creek have a relative distribution similar to sediments, unlike other eclogites'.

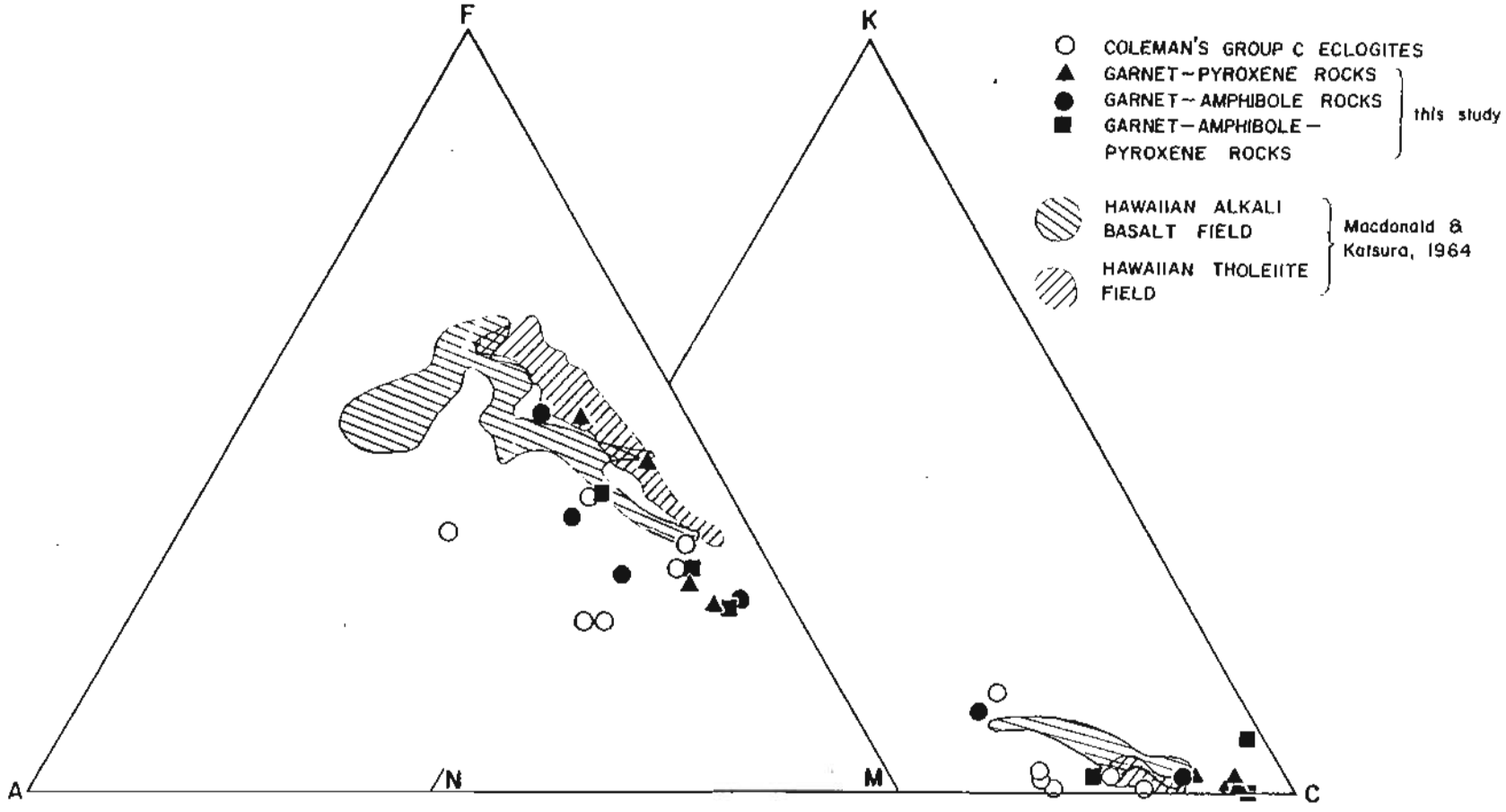

Figure 4. FMA-CNK diagrams illustrating the compositional fields of Hawaiian tholeiites and alkali basalts, with plots of analyzed rocks from the Fairbanks mining district eclogite-facies terrane.

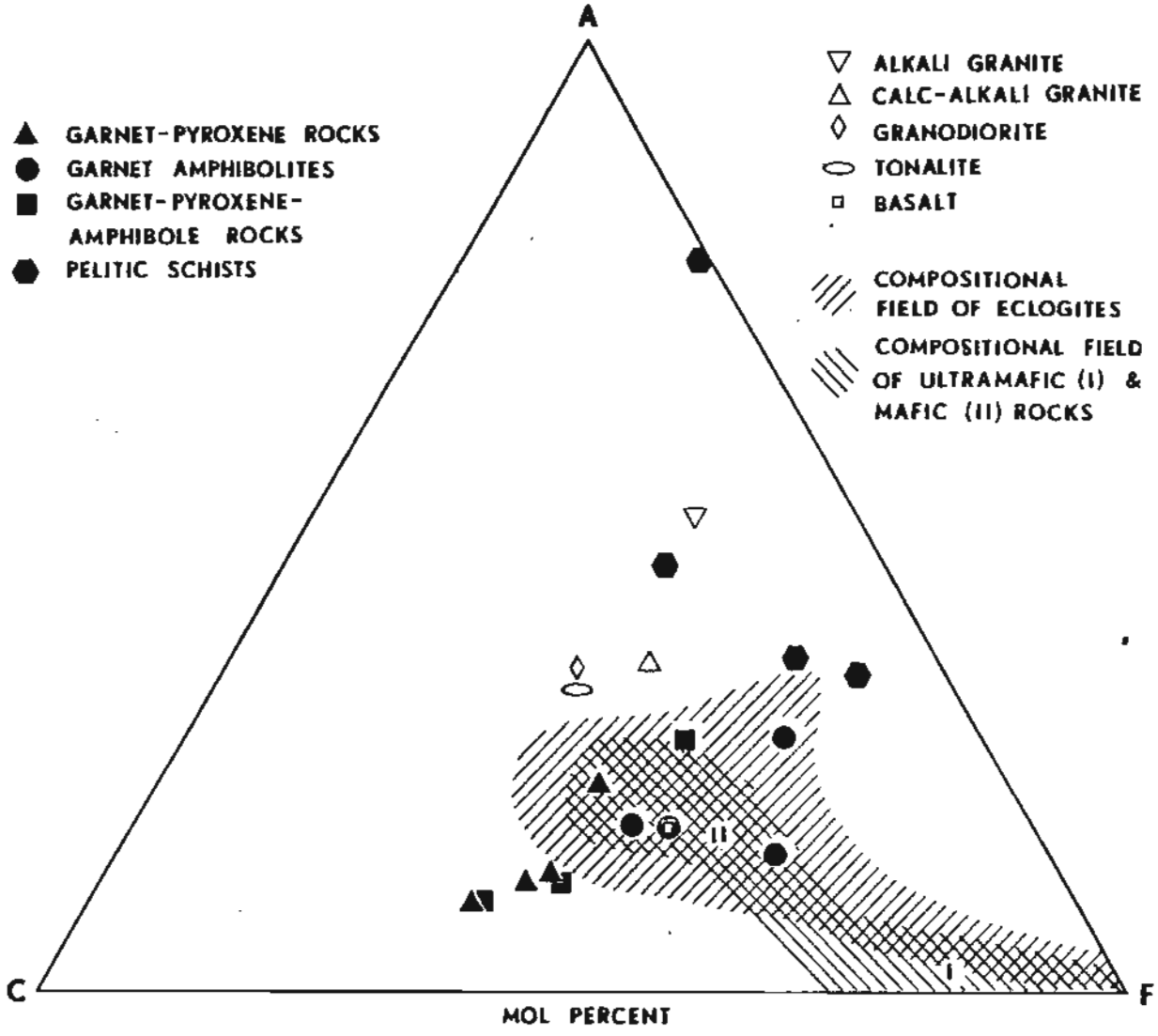

Figure 5. ACF diagram illustrating the compositional fields of eclogites and mafic and ultramafic rocks, and plots of analyzed rocks from the Fairbanks mining district eclogite-facies terrane.

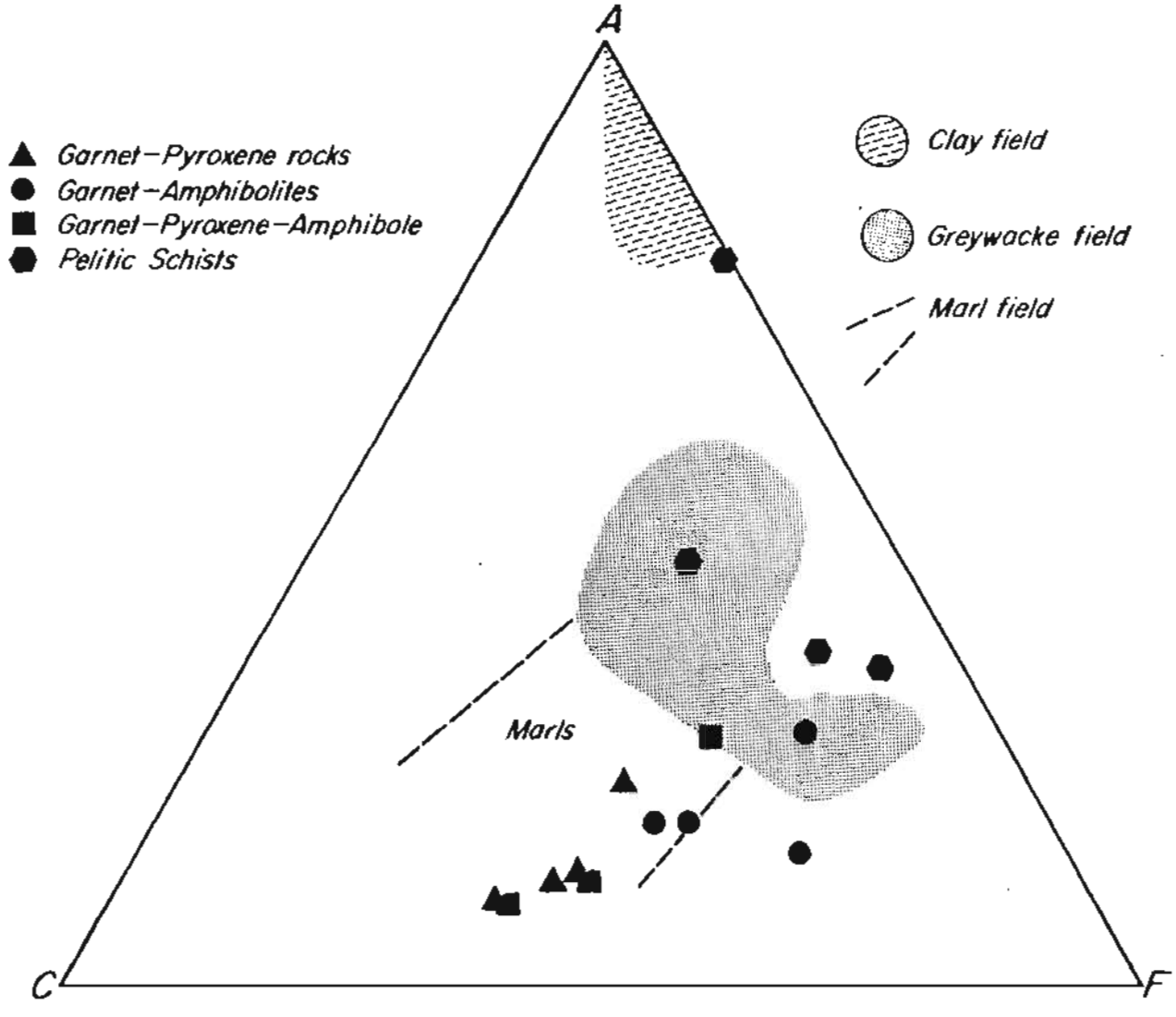

Figure 6. ACF diagram showing the coincidence of eclogite rocks from the Fairbanks mining district and the compositional field of marly sedimentary rocks.

Table 5. Modes of analyzed rocks from the eclogite-facies terrane, Fairbanks mining district, Alaska.

Rock number	Clinopyroxene	Amphibole	Garnet	Calcite	Quartz	Plagioclase	Muscovite	Biotite	Chlorite	Epidote	Apatite	Sphene	Rutile	Opaques	Tourmaline	Phlogopite	Carbonaceous material	Orthite	Unidentified alteration products
F10	- -	- -	0.8	- -	36.1	6.2	40.2	4.0	5.8	- -	- -	- -	- -	4.7	1.6	- -	0.6	- -	- -
F11	- -	- -	2.8	- -	34.8	5.6	13.3	11.3	23.3	- -	0.2	5.3	- -	0.7	1.8	- -	0.3	- -	- -
F29	- -	- -	- -	- -	16.2	10.6	41.6	- -	- -	- -	- -	9.4	6.2	5.1	- -	- -	- -	1.4	7.7
F70	- -	2.6	24.3	- -	32.6	- -	- -	- -	- -	10.2	0.1	- -	6.4	1.2	1.2	- -	- -	- -	20.3
F71	- -	- -	13.2	- -	22.4	5.7	49.9	2.7	- -	2.1	0.3	- -	1.8	0.2	0.3	- -	0.4	- -	1.2
F136	- -	30.4	12.1	15.3	- -	3.2	9.3	18.4	- -	- -	2.2	- -	4.8	2.0	0.9	- -	0.7	- -	1.5
F162	- -	55.8	7.6	- -	- -	6.1	7.1	0.2	7.5	2.8	2.6	- -	7.5	0.3	- -	- -	- -	- -	1.2
F50	16.8	21.5	14.3	28.1	2.1	- -	5.5	- -	- -	3.9	0.5	5.4	- -	0.8	- -	0.7	- -	- -	1.0
F86	13.2	11.2	18.2	- -	34.7	1.7	- -	- -	- -	2.7	0.7	- -	3.8	0.8	- -	2.1	0.5	1.1	8.6
F89	16.3	28.4	23.1	13.4	- -	- -	- -	- -	- -	1.1	10.8	5.8	- -	1.0	- -	- -	- -	- -	- -
F93	12.3	16.8	25.9	26.5	- -	- -	- -	- -	- -	- -	6.2	7.1	- -	3.0	- -	1.1	- -	0.4	- -
F99	5.4	13.3	17.3	- -	25.9	15.2	0.3	- -	- -	18.8	- -	0.2	1.1	- -	0.3	1.4	- -	- -	- -
F39	30.3	4.2	18.8	29.0	- -	- -	0.3	- -	- -	0.3	6.4	5.4	- -	1.1	- -	2.6	- -	1.0	- -
F75	44.3	7.9	8.6	19.4	- -	1.9	- -	- -	- -	8.2	0.7	5.2	- -	1.5	- -	0.9	0.8	0.7	- -
F78	25.7	5.7	11.2	48.7	- -	- -	- -	- -	- -	- -	1.8	2.7	- -	3.2	- -	- -	- -	0.9	- -
F80	46.8	4.0	14.6	12.3	1.8	2.1	- -	- -	- -	3.0	2.1	8.1	- -	1.5	- -	- -	- -	- -	7.1
F92	24.5	7.9	28.3	29.1	- -	- -	- -	- -	- -	0.8	3.9	8.7	- -	1.5	- -	1.7	0.7	0.9	- -
F100	31.1	8.9	23.2	12.1	- -	- -	5.2	- -	- -	0.8	4.6	7.7	- -	3.8	- -	1.3	0.4	- -	0.9
F101	39.2	9.2	21.2	16.2	1.2	- -	- -	- -	- -	1.0	5.6	3.9	- -	1.9	- -	- -	1.2	0.8	2.3
F201	21.7	8.4	7.3	- -	31.1	6.7	- -	- -	- -	4.3	- -	5.9	0.9	0.8	- -	- -	- -	- -	8.2

Radiometric Age Relationships of the Metamorphic Rocks

Metamorphic facies vs apparent potassium-argon ages

The oldest apparent potassium-argon age obtained from metamorphic rocks in the district (478.5 ± 35 m.y.) was determined for an amphibole separated from an eclogitic rock collected from the 6.2 Mi Elliott Highway borrow pit (table 1, map number 11). Although the mineral separate was of excellent quality, the potassium content was quite low (0.166 percent), which would compromise the reliability of the age determination if there was any excess radiogenic argon in the amphibole. Swainbank and Forbes (1975) attempted to clarify the polymetamorphic history of the eclogite-facies rocks by separating and dating coexisting hornblende, biotite, and white mica from a host rock in the 6.2 Mi pit, with the following results:

Phase	% K_2O	Age
Amphibole	0.412	132 ± 8 m.y.
Biotite	6.842	108.5 ± 3.4 m.y.
White mica	4.970	103.5 ± 3.4 m.y.

There is no statistically significant difference in the apparent biotite and white-mica potassium-argon ages, but the apparent cooling age of the amphibole is clearly greater than that of the micas. However, the argon-blocking temperature is appreciably higher for amphiboles vs micas, and the discordance may be due to this factor rather than partial overprinting. The oldest apparent potassium-argon muscovite (166.2 ± 2.2 m.y.) age obtained from the district, however, was also from the eclogite-facies terrane near the old Cleary townsite (table 1, map number 14). The age was determined on a very pure sample, but it is probably a minimum age that has been derived from the partial overprinting of an older crystallization age by the widespread 90-135 m.y. thermal event that accompanied the emplacement of granitic plutons in the district.

To date, only two mineral separates have been submitted to potassium-argon dating from the amphibolite-facies terrane, near the community of Fox (Forbes and Weber, 1982, pl. 1). Hornblende from an amphibolite exposed in the Davidson Ditch, above the marble quarry, produced a potassium-argon age of 245.4 ± 18 m.y. (table 1, map number 10). In this case, the potassium content was much higher than that of the amphibole separated from the eclogitic rock in the 6.2 Mi pit, and the number can be accepted as a minimum crystallization age. However, the possibility of partial overprinting still exists, because muscovite from a coarse-grained garnet-mica gneiss near the Fox Roadhouse produced an apparent potassium-argon age of 126.6 ± 3.7 m.y. (table 1, map number 9).

Mica potassium-argon ages from greenschist-terrane rocks range from 102.5 ± 3.0 m.y. to 141.4 ± 2.0 m.y. (table 1, map numbers 4-8). These data are in agreement with mica potassium-argon ages determined for metamorphic rocks in adjacent areas, where overprinting appears to have been complete. Two attempts were made to apply whole-rock dating to greenschist-facies rocks. Garnet-mica schist from a roadcut near the Chatanika River bridge (table 1,

map number 7) yielded an apparent whole-rock potassium-argon age of 133.1 ± 4.0 m.y.

Apparent whole-rock potassium-argon age relationships along the Elliott Highway

In 1962, Kulp and Forbes collected serial samples from roadcrops along the Elliott Highway, in an attempt to move away from the thermal overprint associated with the emplacement of Tertiary and Cretaceous granitic plutons and the synkinematic metamorphic event responsible for the prograde development of amphibolite- and eclogite-facies rocks in the Fairbanks mining district. At that time, we were not aware of the possibility that the eclogite-facies terrane was a 'tectonic window.' The results of the whole-rock potassium-argon traverse are summarized in table 6. Although the apparent whole-rock potassium-argon ages listed in table 6 do not define a consistent age gradient, there is a tendency toward older apparent ages to the northwest. Based on lithology and structure, the rocks along the road to Livengood do appear to be the protolith for the greenschist-facies metamorphic rocks in the Fairbanks mining district, and metamorphic grade increases from the zeolite facies near Wickersham Dome to lower greenschist facies on the northwest valley side of the Chatanika River. If the whole-rock potassium-argon ages are meaningful, the potassium-argon clock would be chiefly controlled by the cooling age of incipient mica (sericite), which is an ubiquitous phase in the rocks collected along the traverse.

Table 6. Apparent potassium-argon ages of rocks from the Elliott Highway traverse, Fairbanks mining district, Alaska (unpublished analyses by J. Engel).

Sample number	Location	Rock type	Apparent age
LK 8-11-8	Fox Spring house	quartz-mica schist (M)	102.5 ± 3 m.y.
LK 8-11-7	Chatanika River bridge	garnet-mica schist (WR)	133.2 ± 4 m.y.
LK 8-11-6	Mi 20.5	quartz-mica schist (WR)	88.2 ± 3 m.y.
LK 8-11-5	Mi 26.5	quartz-mica schist (WR)	171 ± 31 m.y.
LK 8-11-4	Mi 31 Wickersham Dome	phyllonite (WR)	182.2 ± 5 m.y.
LK 8-11-3	Mi 32 Wickersham Dome	phyllonite (WR)	93.3 ± 4 m.y.
LK 8-11-2	Mi 34 Wickersham Dome	phyllonite (WR)	262 ± 8 m.y.
LK 8-11-1c	Globe Creek quarry	purple slate (WR)	234.2 ± 7 m.y.
LK 8-11-1b	Globe Creek quarry	gray metasiltstone (WR)	477.6 ± 14 m.y.
LK 8-11-1a	Globe Creek quarry	green slate (WR)	281 ± 8 m.y.

M = Muscovite
WR= Whole rock

The 477.6 ± 14 m.y. whole-rock potassium-argon age of the gray slate is within the Cambro-Ordovician interval defined by the 478.5 ± 35 m.y. hornblende age in the eclogite terrane to the southeast, and the rubidium-

strontium muscovite ages discussed below. If, however, the older age is rejected, we are left with two whole-rock ages from the Globe Creek quarry that suggest a possible Permo-Triassic recrystallization event that has been partially obliterated by a thermal disturbance to the southeast toward the Fairbanks mining district. This recrystallization age interval and possible thermal event has also been suggested by potassium-argon and rubidium-strontium mineral and whole-rock ages in the Big Delta Quadrangle (G.D. Eberlein and D.L. Turner, personal commun.).

Previous potassium-argon rubidium-strontium studies

Wasserburg, Eberlein, and Lanphere (1963) and Eberlein (personal commun.) obtained a rubidium-strontium muscovite age of 509 m.y. from a coarse-grained garnet-mica schist near Long Creek, about 20 mi northeast of Pedro Dome. This occurrence appears to be in another 'window' of eclogite-facies terrane that is exposed on the northside of the Chatanika River valley (Forbes and Weber, 1982, pl. 1). Wasserburg, Eberlein, and Lanphere (1963) and Eberlein (personal commun.) also obtained a rubidium-strontium muscovite age of 511 m.y. from a mica schist near Montana Creek on the Steese Highway.

Summary of radiometric age relations

Based on available radiometric age data from the above sources, it is probable that metamorphic rocks of all metamorphic facies in the district were derived from parental rocks of Paleozoic and Precambrian age, or from a protolith that contained clastic material derived from a Precambrian source terrane. The eclogite-facies terrane does appear to have a more complex structural history than the amphibolite- and greenschist-facies terranes. The rubidium-strontium muscovite and potassium-argon hornblende ages suggest a possible Cambro-Ordovician recrystallization event in the eclogite terrane, followed by partial or complete mica overprinting during a subsequent Cretaceous thermal disturbance that was accompanied by the emplacement of granitic plutons. The 240-275 m.y. event that is suggested by the hornblende potassium-argon age from the amphibolite near Fox has also been detected in hornblende potassium-argon ages in the Big Delta Quadrangle, and may represent a significant regional pulse in the thermal history.

In the southeastern part of the Yukon-Tanana Upland, some biotite and hornblende potassium-argon ages are in the 160-190 m.y. range, and are thought to be related to the thermal disturbance accompanying the emplacement of the Mt. Taylor Batholith and related satellitic plutons (Foster and others, 1973). However, hornblende from amphibolite samples in the Big Delta Quadrangle also yielded apparent ages in this interval (D.L. Turner, personal commun.), and the possible effect of such an event on the apparent potassium-argon ages in the Fairbanks mining district is not yet understood.

Cretaceous granitic plutons and their accompanying thermal perturbations in the metamorphic country rock have clearly overprinted (or partially overprinted) the apparent potassium-argon mica ages in the Fairbanks mining district, and the amphiboles in both eclogite- and amphibolite-facies terranes have been partially overprinted by this same disturbance. F.H. Wilson (manuscript in preparation) has recent evidence that suggests that a Cretaceous

regional thermal pulse may have preceded the actual emplacement of the granitic plutons in the district.

PETROLOGY OF THE GRANITIC ROCKS

Granitic rocks were emplaced in the Fairbanks mining district metamorphic rocks during Cretaceous to early Tertiary time. Granitic rock types known to occur in the district include:

- .Hornblende-biotite (± augite) granodiorite and quartz diorite
- .Biotite quartz monzonite
- .Hypersthene-bearing biotite granite
- .Quartz-monzonitic and granitic dike rocks.

Distribution and Cooling Ages

Distribution

Granitic plutons in the district include the Gilmore Dome, Pedro Dome (Pedro, Twin Creek, and Steamboat Creek), and Approach Hill (Fort Wainwright) plutons. Small hypabyssal bodies and dikes occur throughout the district (Forbes and Weber, 1982, pl. 1).

Crystallization age

Table 7 lists radiometric ages that have been determined for granitic plutons in the Fairbanks and adjacent districts. Inspection of the table shows that the crystallization ages of plutons group into three intervals: 115 m.y., 89-95 m.y., and 58-65 m.y.

Although the 58-65 m.y. plutons have overprinted the apparent potassium-argon mineral ages of metamorphic rocks near the contacts, this episode of plutonism does not seem to have been accompanied by a regional thermal event. However, discordant potassium-argon hornblende vs mica ages in metamorphic rocks in the Fairbanks mining district indicate that a pervasive regional thermal event did occur in the 90-120 m.y. interval that may have been associated with the earlier generation of granitic plutons.

Quartz Diorite-Granodiorite

Field relations

The quartz diorite-granodiorite plutons are exposed in three separate, elongate bodies (Forbes and Weber, 1982, pl. 1). The largest extends from Pedro Dome west-southwest approximately 3 mi to the head of Moose Creek Number 2. A second elongate pluton (exposed south of this mass) extends from the head of Fox Creek 3 mi east-northeast into Granite Creek. A third pluton crops out along the Steese Highway, north of the confluence of Twin and Pedro Creeks. These plutons are known as the Pedro Dome, Steamboat, and Steese plutons, respectively (Britton, 1969).

Table 7. Radiometric ages of granitic rocks from the Fairbanks, Circle, Livengood, and Big Delta Quadrangles, Alaska.

Pluton	Quadrangle	Age	References
Pedro Dome (qd)	Fairbanks	(h) 93.0 ± 5.1 m.y.	Swainbank and Forbes (1975)
Pedro Dome (qm)	Fairbanks	(b) 95.3 ± 5.0 m.y.	Forbes, Kulp, and Engel (unpublished)
Approach Hill (gr)	Fairbanks	(b) 117.8 ± 6.0 m.y.	Forbes, Kulp, and Engel (unpublished)
Birch Lake (qm)	Big Delta	(b) 89.3 ± 2.7 m.y. (h) 87.8 ± 2.7 m.y.	Wilson (1976, personal commun., 1977)
Chena Hot Springs (qm)	Circle	(b) 59.7 ± 1.7 m.y.	Biggar (1974)
Tors (Chena Lobe) (qm)	Big Delta	(b) 91.4 ± 3.3 m.y.	Turner (personal commun., 1981)
Granite Tors (qm)	Big Delta	(b+m) 59.2/67.7 m.y.	Wilson (personal commun., 1981)
Mt. Prindle (qm)	Circle	(b) 60.0 ± 1.7 m.y.	Holm (1973)
Circle Hot Springs (gr)	Circle	(b) 62 ± 1.8 m.y.	Wasserburg and others (1963); Wilson and Shew (1981)
Cache Mountain (qm)	Livengood	(b) 60.0 ± 1.7 m.y.	Holm (1973)
Tolovana Hot Spring Dome (qm)	Livengood	(b) 65 ± 2.5 m.y.	Chapman and others (1971)

h = hornblende
b = biotite
m = muscovite
qd = quartz diorite
qm = quartz monzonite
gr = granite

Elongation of the outcrop pattern of the Pedro Dome pluton and the western part of the Steamboat pluton is concordant with the most recent structural trend in the area. However, the Steese pluton and the eastern lobe of the Steamboat pluton are apparently discordant to this trend.

In the field it is difficult to distinguish quartz-dioritic vs granodioritic variants. The color varies locally from very light gray to medium gray. Grain size is generally less than 1 mm but may be as much as 2-3 mm.

Contacts along the margins of the Steamboat and Steese plutons were sheared, and the marginal phases of the plutons were hydrothermally altered. Quartz-monzonitic dikes have also been intruded along these shear zones. Exposed contacts are characteristically defined by intense weathering that produces a rusty-brown color and a granular disintegration of the rock that produces grus.

Petrography

Texturally, the quartz diorite-granodiorite plutons have a fine- to medium-grained granitic texture. Flow structures have been noted in the Steese and Steamboat plutons, as defined by subparallel alignment of plagioclase laths and mafic minerals.

Subhedral to euhedral plagioclase laths comprise up to 45 percent of the rock. The plagioclase composition, including zonal variations, ranges from An_{86} (core maximum) to An_{30}. Plagioclase zonation is characterized by calcic cores, intermediate zones, and sodic rims, although all three zones are rarely present in a single grain. Unzoned crystals usually have a composition equivalent to the intermediate zone. Microphenocrysts of more calcic plagioclase as well as more sodic, interstitial plagioclase crystals are also present.

Potassium feldspar (orthoclase) is anhedral and interstitial and micrographic intergrowths with quartz are common. Most orthoclase appears to be homogeneous, although some grains show possible exsolution textures. Carlsbad twins are commonly developed in the larger orthoclase grains, and plagioclase blebs are frequent inclusions. Late, discordant veinlets of quartz and/or orthoclase occur at many localities.

Quartz is typically anhedral and interstitial, and apatite and zircon inclusions are common. Rutilated quartz also occurs. Quartz often shows strained extinction and anomalous biaxial optic angles.

Subhedral biotite comprises 10 to 20 percent of the rocks and occurs as a primary mineral and as an alteration product of hornblende. Zircon inclusions produce pleochroic halos in the biotite. Biotite is commonly altered to chlorite and less frequently to epidote (pistacite).

Green hornblende is present as a reaction product from pyroxene, and twinning is common. The hornblende is subhedral to anhedral. Infrequently it is pseudomorphous after pyroxene. Occasionally the cores of hornblende crystals have been altered to a fibrous mass of tremolite-actinolite.

Pyroxene in the rocks includes both augite and hypersthene. Augite occurs as a minor phase in most specimens, or may be absent. Hypersthene is present when the modal percentage of pyroxene is high (8 to 12 percent), and it never appears without coexistent augite. Hypersthene appears to have crystallized earlier than augite, and it is more susceptible to the hornblende reaction. Pyroxene is subhedral and usually mantled by hornblende reaction rims. Both pyroxenes tend to form glomeroporphyritic clusters. If one or both of the pyroxenes are relatively abundant, there is a corresponding decrease in hornblende.

Accessory (< 1 percent) minerals include magnetite, sphene, apatite, zircon, and epidote (pistacite). Magnetite, sphene, and epidote are usually closely associated with the alteration of mafic minerals. Orthite is a rare accessory.

Quartz Monzonite

Field relations

Quartz monzonite stocks and dikes are exposed throughout the Pedro Dome area. They are exposed in the interstream divide between the heads of Fox and Flume Creeks and along the Steese Highway near Twin and Skoogy Creeks. A relatively large mass of quartz monzonite is also exposed in the Gilmore Dome area (Forbes and Weber, 1982, pl. 1).

The quartz monzonite was definitely emplaced later than the quartz diorite-granodiorite. Local structure, specifically shear and contact zones, appears to have influenced the shape and emplacement of the quartz monzonite plutons. Terminal lobes of these plutons are truncated by numerous dikes and veins, as exposed in the Fox Creek area and along the Steese Highway near Skoogy Creek.

The pluton located near the confluence of Skoogy and Twin Creek (Twin Creek pluton) is a typical medium- to coarse-grained quartz-monzonite porphyry. It weathers to a light-brown color and is light gray to white in fresh samples. Small pegmatitic veinlets, emplaced parallel to joint surfaces, have been noted in several areas. The quartz monzonite pluton located at the head of Fox Creek (Fox Creek pluton) is characterized by abundant quartz, granular texture, and low mafic content. It weathers to a buff color, and in fresh samples it is nearly white. The pluton located at the head of Flume Creek (Flume Creek pluton) occurs as a fine-grained porphyry that weathers to a reddish-brown color and as a second phase that appears to be a medium-grained equivalent of the Fox Creek pluton.

Petrography

The quartz-monzonitic rocks are composed of phenocrystal and glomeroporphyritic quartz, potassium feldspar, and plagioclase in a fine- to medium-grained granular matrix. Representative modal analyses are shown in table 8.

Subhedral to euhedral plagioclase comprises up to 36 percent of the quartz monzonite variants, and is more sodic than the plagioclase in the

Table 8. Modes of representative specimens of quartz diorite-granodiorite and quartz monzonite from the Fairbanks mining district, Alaska (Britton, 1969).

	Granodiorite-quartz diorite						Quartz monzonite	
Mineral	ECPD-25 (%)	ECPD-35* (%)	ECPD-36 (%)	ECPD-205* (%)	ECPD-45 (%)	ECPD-2 (%)	ECPD-72 (%)	ECPD-64 (%)
Plagioclase	33	41	37	35	39	45	38	26
Quartz	28	22	19	26	19	11	34	26
Potassium feldspar	14	14	10	8	8	6	26	38
Biotite	14	12	18	21	16	21	3	tr.
Hornblende (including uralite)	10	11	7	10	5	13		
Clinopyroxene (augite)	- -	- -	3	1	7	1		
Orthopyroxene (hypersthene)	- -	- -	5	- -	5	- -		
Accessory minerals	1	1	2	1	2	1	1	1
K-feldspar/plagioclase + K-feldspar	29.8	25.4	21.3	18.8	17.0	11.7	41.0	59.4

*See table 9 for whole-rock analyses.

quartz diorite-granodiorite plutons. The anorthite content of the plagioclase ranges from An_{47} to An_{23}. Compositional zonation is typically present and is normal. Calcic cores of phenocrysts are generally in the compositional range An_{35} to An_{45}, and the more sodic outer zones range from An_{33} to An_{23}. Unzoned crystals and groundmass grains are usually equivalent to the more sodic rims of the zoned phenocrysts. Well developed sericitic alteration is common in the plagioclase grains, with lesser amounts of calcite and epidote.

Quartz phenocrysts are typically subhedral to euhedral, with abundant inclusions and bubble trains. Quartz in the matrix is anhedral. Both varieties exhibit strained extinction.

Orthoclase and streaky perthite compose up to 38 percent of the rocks. Potassium feldspar is usually in the form of subhedral phenocrysts, but also occurs as anhedral grains in the matrix. Plagioclase and quartz inclusions are common in the potassium-feldspar phenocrysts. Incipient microcline was noted along fractures in potassium-feldspar phenocrysts and as small grains in the matrix.

Biotite occurs in minor amounts (2-3 percent) as the dominant mafic mineral. It is usually subhedral, with strong absorption. Pleochroic halos around zircon inclusions are common. Quartz is sometimes enclosed by highly altered biotite, indicating that the biotite was corroded before or during crystallization of the quartz. Biotite is typically altered to chlorite.

Magnetite, hornblende, apatite, sphene, and zircon are all accessory minerals in the quartz monzonite; orthite also occurs as a rare accessory. Epidote (clinozoisite) and calcite are usually present as the result of feldspar alteration. Secondary magnetite and sphene have apparently developed from the chemical breakdown of mafic minerals.

Altered granitic rocks

A linear zone of hydrothermally altered quartz diorite traverses the Pedro Dome pluton from the west flank of Pedro Dome to the head of Steamboat Creek. This zone appears to be localized along a shear zone, based on the presence of slickensides and cataclastic structures. The rocks in this zone have altered to rusty brown or chalky white and are very conspicuous in outcrop.

The original igneous texture is discernable in some thin sections, but has been obliterated by severe alteration in others. Feldspars have been almost totally altered to clays, and the mafic minerals have altered to ferruginous material.

Whole-rock Chemistry

Inspection of whole-rock and norm analyses (tables 9, 10) of granitic rocks from the Fairbanks mining district shows that the granitic suite is dominantly potassic (potassium exceeds sodium in all analyzed rocks). Additionally, five analyzed rocks (samples 1-4,6) are corundum normative, and

Table 9. Whole-rock analyses of granitic rocks from the Fairbanks mining district, Alaska

Sample number	Quartz monzonite 1	Quartz monzonite 2	Quartz monzonite 3	Quartz monzonite 4	Granodiorite 5	Granodiorite 6	Granodiorite 7	Peralkaline granite 8	Monzonite 9
	Porphyry dikes		Fox Creek	Steese	Steamboat	Creek	Steese	Approach Hill	Harding Lake
Oxide (wt.%)	ECPD-46[a]	ECC-1-228[a]	ECP-4[a]-16	ECC-2[a]-174	ECPD[a]-205	ECPD[a]-35	ECC-4[a]-26	AP-1[b]	HL-1[b]
SiO_2	73.62	69.85	70.96	74.19	61.63	65.09	59.67	78.47	54.35
TiO_2	0.02	0.21	0.03	0.11	0.85	0.66	1.03	tr.	0.76
Al_2O_3	14.35	15.63	16.27	13.64	15.53	16.02	17.17	10.94	17.09
Fe_2O_3	0.65	0.55	1.19	0.05	1.92	0.06	1.17	0.63	0.97
FeO	0.82	3.84	1.22	1.11	4.95	4.15	5.76	0.48	7.61
MnO	0.03	0.06	0.01	0.05	0.13	0.11	0.13	0.03	0.14
MgO	0.11	0.64	0.23	0.34	2.72	2.04	2.56	0.86	4.90
CaO	1.04	2.07	0.23	1.46	5.90	4.52	6.33	0.86	8.00
Na_2O	2.84	2.48	2.98	3.69	2.07	2.53	2.13	3.67	2.13
K_2O	5.36	3.56	5.46	3.80	2.67	3.50	3.16	4.79	3.23
H_2O^+	0.91	1.05	1.30	0.64	1.32	1.06	1.12	0.09	0.29
H_2O^-	0.67	0.50	0.50	0.54	0.63	0.26	0.13	0.01	0.13
P_2O_5	0.01	0.10	0.02	0.03	0.21	0.21	0.31	nil	0.26
Totals	100.43	100.54	100.40	99.65	100.48	100.21	100.67	100.83	100.86

[a]Tadashi Asari, analyst.
[b]H. Haramura, analyst.

Table 10. Igneous norms (Shaw, 1969) for chemically analyzed granitic rocks from the Fairbanks mining district, Alaska.

Sample number	1	2	3	4	5	6	7	8	9
Quartz	32.04	32.27	29.77	32.01	20.36	20.66	14.47	33.95	2.43
Orthoclase	32.45	21.69	33.03	22.99	16.35	21.16	19.10	28.37	19.32
Albite	26.13	22.96	27.40	33.92	18.80	23.25	19.57	31.49	19.37
Anorthite	5.22	9.92	1.03	7.22	26.36	21.55	28.61		27.88
Corundum	2.25	4.70	5.69	0.98		0.40			
Diopside					2.05		1.16	3.42	8.47
Hypersthene	1.17	7.36	1.71	2.61	12.31	11.54	13.69	1.32	19.87
Acmite								1.23	
Ilmenite	0.03	0.03	0.04	0.16	1.23	0.94	1.47	0.01	1.07
Magnetite	0.70	0.59	1.27	0.05	2.08	0.06	1.25	0.20	1.03
Apatite	0.02	0.02	0.04	0.06	0.46	0.45	0.66		0.55

one (sample 8) is acmite normative; these parameters classify the rocks as members of the alkaline suite (table 10).

Samples 5 and 7 are mafic-rich variants from the quartz diorite-granodiorite suite from Pedro Dome, and sample 9 is a mafic-rich monzonitic dike rock from the Harding Lake area that may not be genetically related to the granitic rocks in the Fairbanks mining district.

Plots on the FMA-CNK (fig. 7) and normative diagrams (fig. 8) indicate that samples 1, 3-4, and 8 are the most alkalic variants in the suite, and according to the criteria developed by Chappell and White (1974), these rocks and samples 2 and 6 may be anatectic granites derived from partially melted crustal metasediments (table 11). Such granites are often associated with tin and tungsten mineralization and are of special interest to studies of the economic mineral potential of the Fairbanks mining district.

The normative (fig. 8) and FMA-CNK (fig. 7) diagrams reinforce the petrologic kinship between the quartz-dioritic and granodioritic variants, and the Ca-depleted composition of the hypersthene-bearing peralkaline granite from Approach Hill. The An-Ab-Or diagram also confirms the genetic relationship between sample 1, a quartz-monzonitic dike rock from Pedro Dome, and sample 4, a coarse-grained quartz monzonite exposed in a roadcut along the Steese Highway.

Trace- and Minor-element Chemistry

In addition to the whole-rock chemical analyses, spectrographic data were also obtained for trace minor- and major-element content of eight representative samples from the Pedro Dome plutons. Concentrations of the various elements were spectrographically determined with a Jarrell-Ash 1.5-m-grating spectrograph. Reported values are based on the U.S. Geological Survey's six-step method of comparison in which concentrations are reported to the nearest number in a series of standards prepared by that agency. Results are considered precise to ±22 percent of the reported value at the 1σ level. Analytical work was performed by D.L. Stevens in the University of Alaska Mineral Industry Research Laboratory.

Values obtained for these analyses are listed in table 12; data contain several trace-element anomalies that may be related to mineralization in the district:

- Anomalously high silver, copper, molybdenum, and lead in quartz monzonite at the head of Fox Creek.
- Anomalously high lead in most granitic variants in the Pedro Dome area.
- Anomalously high copper, vanadium, zinc, and lead in altered quartz diorite zone on Pedro Dome.

Argentiferous galena has been extracted from mineralized fracture and shear zones in the Steamboat Creek granodiorite, and galena-sphalerite-chalcopyrite veins have been mined in the granodiorite-quartz monzonite at the head of Fox Creek. Trace molybdenite can be seen in walls of the Silver Fox (Busty Belle) adit driven into the Fox Creek granodiorite.

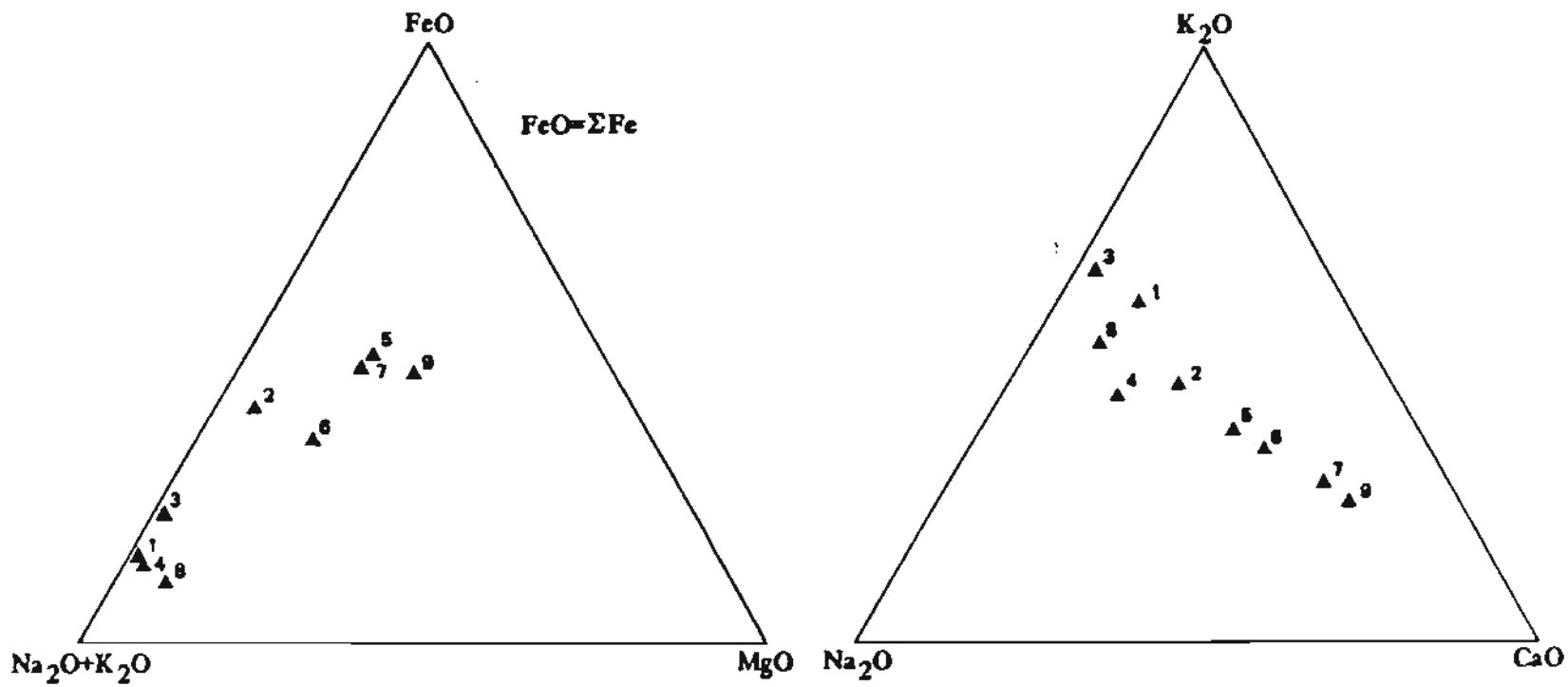

Figure 7. FMA-CNK diagrams with plots illustrating the comparative composition of granitic rocks from the Fairbanks mining district, Alaska (see table 8 for source analyses).

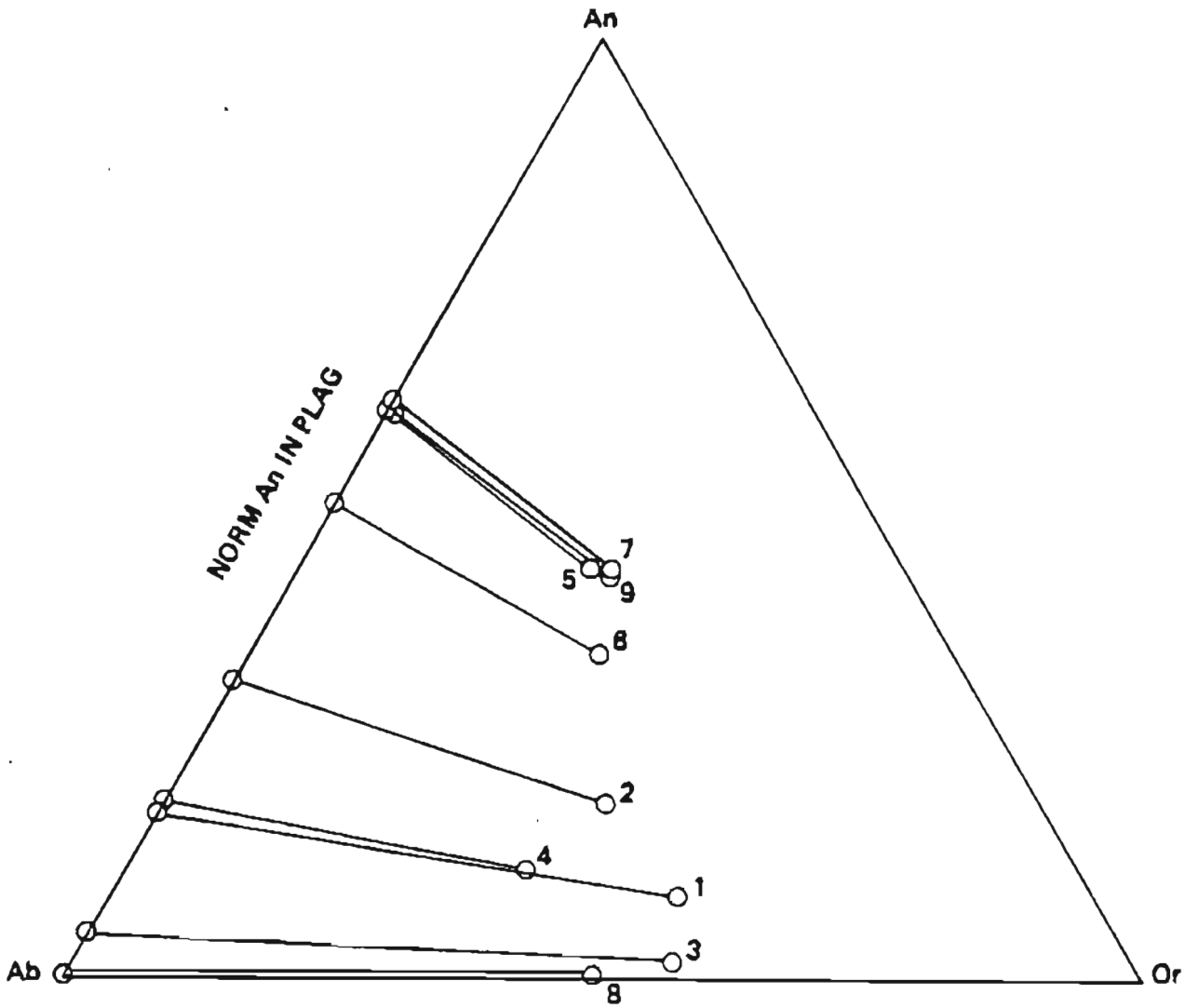

Figure 8. Normative albite-orthoclase-anorthite diagram---with tie lines between plots of normative whole-rock and constituent plagioclase composition---for analyzed granitic rocks from the Fairbanks mining district, Alaska.

Table 11. Chemical and mineralogical parameters for the discrimination of 'S' versus 'I' granite types (Chappell and White, 1974), applied to analyzed granitic rocks from the Fairbanks mining district.

Parameters	Sample numbers								
	1	2	3	4	5	6	7	8	9
Relatively low sodium vs vs potassium	S	S	S	S	S	S	S	S	S
Mol. $Al_2O_3/Na_2O+K_2O+CaO)$ 1.1	S	S	S	S	S	S	S	S	S
1 percent normative corundum (acmite) vs diopside	S	S	S	S	I	S	I	S	I
Biotite vs hornblende	S	S	S	S	I	S	I	S	I

Intrusive Sequence and Crystallization History
(from Britton, 1969)

The Pedro Dome plutons appear to be a genetically related group of intrusives emplaced during the final stages of the latest recognizable tectonic event. The composition of the plutons ranges from quartz diorite to granodiorite; subordinate quartz monzonite occurs as small stocks and dikes. The compositional variation makes it difficult to treat a particular pluton as strictly quartz dioritic or granodioritic. However, the Pedro Dome pluton is dominantly composed of quartz diorite, the Steese pluton is granodioritic in composition, and the Steamboat pluton is transitional between quartz diorite and granodiorite. The eastern part of the Steamboat mass is granodioritic while the western extension is more appropriately termed quartz diorite.

It is reasonable to conclude that the exposed portions of the quartz diorite-granodiorite represent contact phases of an underlying pluton that has only recently been unroofed. The homogeneous fabric of the plutons lends support to this view. The granodiorite-quartz diorite variants of the plutons may be related to the depth of burial of the original intrusive mass. The granodioritic plutons are located 500 to 1,000 ft topographically lower than the quartz-diorite phase on Pedro Dome. This may be an important consideration in regard to the western vs eastern lobes of the Steamboat pluton.

The emplacement of the quartz diorite, and in particular the Pedro Dome pluton, appears to have been a rather passive injection of the magma into the core of the Pedro Dome anticlinorium, because the elongate outcrop pattern approximately parallels the axis of the anticlinorium. The passive nature of the injection is also indicated by a lack of shearing along the contacts. The granodioritic plutons are elongate parallel to local shear dislocations that occur along the contact zones of these plutons. Flow structures, as previously mentioned, occur only in the granodioritic masses. These relations support the view that the more alkalic plutons were emplaced in a semi-consolidated state while shearing was still active, probably when one or more of the active shears breached reservoirs or apophyses of unconsolidated melt and allowed late differentiates of the cooling magma to move out along these shear zones. This differentiate was probably composed of crystalline material

Table 12. Spectrographic analyses of representative samples from the Pedro Dome plutons, Fairbanks mining district, Alaska.

	Quartz monzonite porphyry dike		Quartz monzonite Fox Creek	Quartz monzonite Steese	Granodiorite Steamboat pluton		Quartz diorite	Altered granitic material
Element	ECPD-46	ECC-1-22B	ECP-4-16-67	ECC-2-124-68	ECPD-205	ECPD-35	ECC-4-26-68	ECPD-21-68
Fe%	0.80	4.07	2.24	1.03	7.88	4.67	8.62	8.09
Mg%	0.048	0.51	0.16	0.27	2.92	1.43	1.93	0.92
Ca%	0.69	1.97	0.13	1.23	4.67	3.27	5.19	0.91
Ti	200	2130	280	1100	7590	5290	8680	8680
Mn	196	690	130	980	1830	980	1920	3060
Ag	n.d.	n.d.	80	n.d.	n.d.	n.d.	n.d.	n.d.
As	n.d.	n.d.	n.d.	n.d.	n.d.	n.d.	n.d.	n.d.
Au	n.d.	n.d.	n.d.	n.d.	n.d.	n.d.	n.d.	n.d.
B	5	5	67	5	12.9	5	19	17.8
Ba	680	1000	930	505	930	860	860	115
Be	n.d.	n.d.	n.d.	n.d.	n.d.	n.d.	n.d.	n.d.
Bi	n.d.	n.d.	n.d.	n.d.	n.d.	n.d.	n.d.	n.d.
Cd	n.d.	n.d.	n.d.	n.d.	n.d.	n.d.	n.d.	n.d.
Co	n.d.	n.d.	n.d.	n.d.	n.d.	n.d.	n.d.	n.d.
Cr	10	18	33	10	72	31	36	82
Cu	1.8	146	126	27.7	17.2	1.8	112.4	39
Ge	n.d.	n.d.	n.d.	n.d.	n.d.	n.d.	n.d.	n.d.
In	n.d.	n.d.	n.d.	n.d.	n.d.	n.d.	n.d.	n.d.
La	n.d.	n.d.	n.d.	n.d.	n.d.	n.d.	n.d.	n.d.
Mo	n.d.	n.d.	5.9	n.d.	4		n.d.	7
Nb	n.d.	n.d.	n.d.	n.d.	n.d.	n.d.	n.d.	n.d.
Ni	5	5	5	5	5	5	9.4	19.8
P	n.d.	n.d.	n.d.	n.d.	n.d.	n.d.	n.d.	n.d.
Sb	n.d.	n.d.	n.d.	n.d.	n.d.	n.d.	n.d.	n.d.
Sc	n.d.	n.d.	n.d.	n.d.	19.7	8.9	17.3	18.8
Sn	n.d.	n.d.	n.d.	n.d.	n.d.	n.d.	n.d.	n.d.
Sr	n.d.	330	n.d.	330	450	350	420	n.d.
V	10	10	10	10	120	67	127	148
W	n.d.	n.d.	n.d.	n.d.	n.d.	n.d.	n.d.	n.d.
Y	n.d.	n.d.	n.d.	n.d.	n.d.	n.d.	n.d.	n.d.
Zn	n.d.	n.d.	n.d.	n.d.	n.d.	n.d.	n.d.	133
Zr	34	115	70	43.5	157	242	1260	185
Pb	9	35.1	69.7	34.0	72.3	9	27.9	17.2

and an alkali-rich fluid that lubricated the movement of the crystal mush. As the crystal-fluid mixture moved further from the magma chamber, filter pressing may have become important. The residual fluids were slowly forced out of the crystal interstices and migrated toward the sheared margins. Flow structures were preserved only along the quickly chilled contacts; the interior of the mass retained sufficient heat to re-equilibrate and obscure the flow structures.

The relationship between the quartz diorite-granodiorite phases of the intrusives and the quartz monzonites is not as readily apparent. The small dikes that were intruded along the contact zones of the quartz diorite-granodiorite plutons may be equivalent to the alkali-rich derivatives that were forced into the shear zones by filter pressing. However, the stock-size masses require considerably more material than would be available from this process. A reasonable conclusion is that these quartz monzonites were the product of a long period of differentiation within the parental magma chamber. This differentiation produced an alkali and volatile-rich fluid that moved along preferential shears and contact zones in the same manner as the granodiorite magma. This event was definitely later than intrusion of the granodiorite, as evidenced by quartz-monzonite veins that cross-cut the granodiorite in outcrops along the Steese Highway. The numerous quartz monzonite dikes and veins of the larger masses indicate that the quartz monzonite magma was very mobile. A high volatile content is also indicated by pegmatitic veinlets of quartz and potassium-feldspar within the quartz monzonite stocks. The lack of noticeable brecciation or thermal effects in the granodiorite adjacent to cross-cutting quartz monzonite dikes and veins indicates that the intrusion of the quartz monzonite followed the granodiorite before the complete consolidation of the granodiorite.

Crystallization of the quartz diorite-granodiorite plutons closely followed the relations outlined by Bowen's reaction series (Bowen, 1928). Pyroxene was the first to crystallize, closely followed by calcic plagioclase. The augite and hypersthene have been preserved only in the contact phases where crystallization was accelerated and early differentiates were not removed by reaction relations. In most cases, the pyroxene reacted with the later phase of the magma to form hornblende, as evidenced by hornblende rims on relict pyroxene and by the near absence of hornblende when pyroxene is abundant. Primary crystallization of hornblende probably also occurred at this time. Biotite closely followed or was perhaps contemporaneous with the pyroxene-hornblende reaction. During this time, plagioclase was also precipitating and becoming more sodic.

The final phase of crystallization was characterized by late-stage silica and alkali-rich fluids that produced interstitial quartz, potassium-feldspar, and sodic plagioclase. Some eutectic crystallization of quartz and potassium-feldspar also occurred in this final stage, as evidenced by graphic intergrowths in the late interstitial fabric.

The experimental work of Jahns and Burnham (1957) may explain crystallization of the quartz monzonite. Jahns and Burnham (1957) found that the separation of an aqueous phase from a melt---through the process of second boiling---produced a marked increase in the size of crystalline material precipitated

from a quartz, potassium-feldspar, and sodic plagioclase mixture. This increase in grain size is due to the promotion of rapid and selective transfer of silica, alumina, and alkalis by diffusion through the aqueous phase brought about by second boiling. This process is evidently necessary for the growth of large crystals. Crystallization is concomitant in both the aqueous and silicate phases. The second boiling may occur with a decrease in pressure and allow the aqueous portion of a melt to become subcritical with subsequent separation into separate phases (vapor and liquid).

Second boiling may have occurred, in the case of the Pedro Dome quartz monzonites, by the pressure decrease that occurred when the quartz monzonite magma was removed from the parent magma reservoir. This would result in the precipitation of large phenocrysts of quartz, potassium feldspar, and sodic plagioclase. After emplacement, the aqueous phase probably escaped along fractures and shear zones as a hydrothermal fluid.

CONTACT METAMORPHIC ROCKS

Granitic plutons were emplaced in the greenschist- and amphibolite-facies terranes in the Fairbanks mining district during a time interval ranging between 58 and 124 m.y. B.P. (table 7). The larger plutons, including the Pedro Dome granitic complex and the Gilmore Dome pluton, are surrounded by contact-metamorphic aureoles that extend 1,600 ft or more into the surrounding schists. The schists display characteristic hornfelsic fabrics and assemblages caused by the superimposed thermal overprint accompanying the emplacement of the granitic plutons. Proximity to the actual intrusive contact and whole-rock chemical composition are the variables that control the superimposed mineral assemblages and fabrics.

Gilmore Dome Contact Zone

The Gilmore Dome pluton is emplaced in schists that appear to include the greenschist-facies variants and a thin veneer of amphibolite-facies rocks that are positioned on the northwest limb of the Gilmore antiform. Calc-magnesian rocks adjacent to the contact near the summit of Gilmore Dome have been recrystallized under conditions of the pyroxene-hornfels facies and have developed assemblages that include diopside, vesuvianite, and garnet. Pelitic rocks in the same zone display typical hornfelsic fabrics dominated by biotite rosettes and andalusite porphyroblasts. Some contact metasomatism has apparently occurred near the contact zone, because the calcareous hornfelses also contain trace amounts of hedenbergite, fluorite, scheelite, and cassiterite.

Pedro Dome Contact Zone

The Pedro Dome composite pluton includes quartz-dioritic, granodioritic, and quartz-monzonitic phases (Forbes and Weber, 1982, pl. 1) and intrudes greenschist-facies metamorphic rocks. The contact aureole is more narrow (about 328 ft) than that surrounding the Gilmore Dome pluton and is chiefly defined by hornfelsed quartzites, quartz-mica schists, and greenschists upgraded to amphibolites. The quartz-mica schists have developed biotite rosettes that have grown across the crystallization foliation and display the

resistance to the hammer that characterizes hornfelsed rocks. Incipient andalusite has also been detected in some of the biotite hornfelses. A large lens of greenschist is cut by the intrusive contact on the north flank of Pedro Dome. Near the contact, the greenschists have been upgraded to amphibolite where the former actinolite has been upgraded to green hornblende and leucoxene to sphene.

Approach Hill Contact Zone

Adjacent to the Approach Hill pluton, calc-schists have been recrystallized under pressure-temperature conditions of the pyroxene-hornfels facies. Garnet, vesuvianite, diopside, and wollastonite have selectively recrystallized along suitable compositional layers where the reactants calcium, magnesium, aluminum, and silica were available.

PETROLOGY OF THE MAFIC IGNEOUS ROCKS

Basalts

Distribution and field relations

Outcrops of basaltic rocks have been mapped at several localities in the Fairbanks mining district, including Birch Hill, Sage Hill, Lakloey Hill, Browns Hill, Millers Bluff, and Fairbanks Creek (Forbes and Weber, 1982, pl. 1). Basalts exposed on Birch and Sage Hills include pillow lavas and palagonite breccias that indicate subaqueous emplacement. Field relations on Lakloey Hill include an unconformity defined by basalt flows that overlie eroded schists and a younger and overlying intraflow contact zone that contains silicified wood.

Fairbanks Creek basalts are associated with coal-bearing sandstones and conglomerates that are believed to be of middle or late Eocene age. A Late Cretaceous whole-rock potassium-argon age (82.2 ± 3.6 m.y.) (table 1, map number 1) was determined for a pillow-bearing flow unit on Birch Hill, but silicified Metasequoia remains recovered from breccia at the base of Birch Hill by Péwé (Péwé and others, 1976b) are believed to be of early or middle Tertiary age. The actual age of the basalt is unclear, but it is generally regarded as Tertiary because of the accompanying sediments.

Petrology

Based on the work of Furst (1968) and others, the rocks are olivine basalts that are chemically transitional between tholeiites and alkali basalts. The mineralogy of the basalts from the Fairbanks mining district is characterized by olivine phenocrysts in a groundmass of plagioclase, augite, olivine, and glass. Whole-rock chemistry of representative basalts from Birch Hill and Millers Bluff is shown in table 13. Modal analyses of basalts from the six localities are listed in table 14. A comparison of the TiO_2-SiO_2 content of the analyzed basalts to that of worldwide basalts from various tectonic settings, as compiled by Furst (1968), is shown in figure 9. These data indicate that the rocks are compositionally similar to tholeiitic basalts erupted in island-arc or intracontinental tectonic settings.

Table 13. Chemical analyses of Fairbanks mining district basalts and average chemical compositions of tholeiitic and alkalic basalts (from Furst, 1968).

Oxides (wt.%)	Birch Hill[a]	Millers Bluff[a]	Average alkali basalt[b]	Average tholeiitic basalt[b]
SiO_2	50.50	52.22	45.78	50.83
TiO_2	1.43	1.19	2.63	2.03
Al_2O_3	15.13	16.91	14.64	14.07
Fe_2O_3	3.81	0.85	3.16	2.88
FeO	7.32	7.61	8.73	9.06
MnO	0.08	0.13	0.20	0.18
MgO	5.60	6.91	9.39	6.34
CaO	8.82	8.20	10.74	10.42
Na_2O	3.50	2.83	2.63	2.23
K_2O	1.54	1.17	0.95	0.82
P_2O_5	0.34	0.03	0.39	0.23
H_2O^+	1.79	1.96	0.76[c]	0.91[c]
H_2O^-	0.23	0.14		
Total	100.09	100.01	100.00	100.00

[a]H. Matsumoto, analyst.
[b]Nockolds (1954)
[c]Total H_2O

Table 14. Modal analyses of basalts from the Fairbanks mining district, Alaska (from Furst, 1968).

Sample locality	Sample number	Olivine	Plagioclase	Augite	Magnetite	Glassy matrix
Birch Hill	FBB-22C	11.5	19.9	- -	- -	68.6
	No. 12	9.5	24.0	- -	- -	66.5
Sage Hill	FBS-1A	10.1	19.9	- -	- -	70.0
Lakloey Hill	FBL-11A	14.3	27.4	- -	- -	58.3
Browns Hill	FBbr-5C	14.5	38.5	2.4	2.1	43.5
Millers Bluff	FBM-3	8.2	43.1	17.4	3.5	27.6
	FBM-14	7.2	40.5	15.5	2.4	34.5
	No. 10	11.0	49.3	12.2	4.9	22.3
Fourth of July Hill	FBF-2	15.6	35.8	9.8	3.2	35.6
	FBF-11	18.9	48.6	12.0	3.2	17.3

Structural implications

The Birch Hill basalts appear to be preserved in a downthrown fault block, and the Fairbanks Creek basalt-sedimentary sequence may have a similar origin. Coal-bearing Tertiary rocks are known to occur in downthrown fault blocks elsewhere in the Yukon-Tanana Upland.

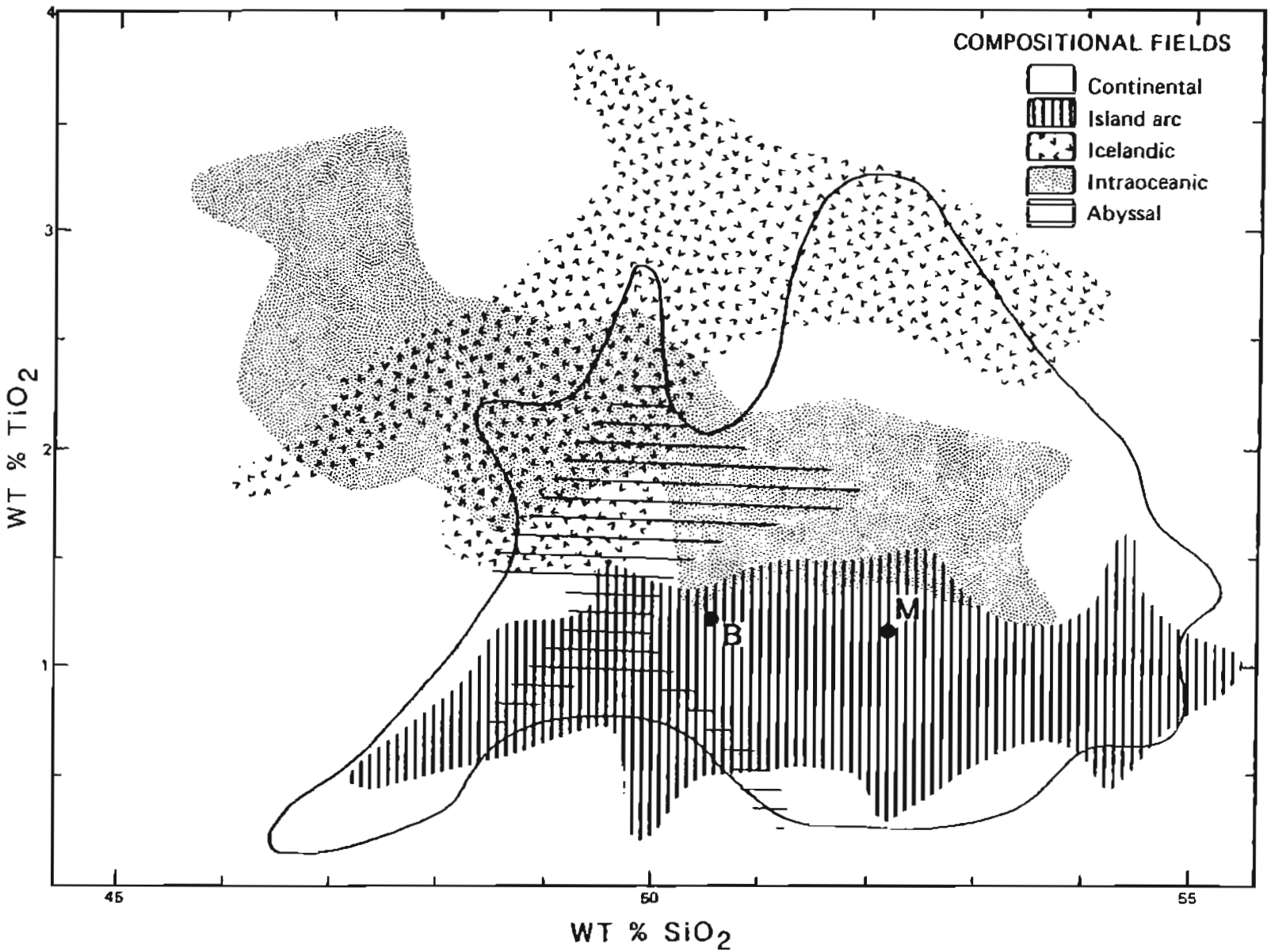

Figure 9. TiO_2-SiO_2 variation diagram showing tholeiitic-basalt compositional provinces and plots for the analyzed basalts from Birch Hill (B) and Millers Bluff (M) (after Furst, 1968).

Ultramafic Rocks

H.D. Pilkington (unpublished) discovered several small ultramafic dikes exposed in roadcuts on the upper section of the Gilmore Dome road. The dike rocks are highly serpentinized, with abundant relict olivine. The parent rocks were probably peridotite. To date, ultramafic plutons have not been discovered in the Fairbanks mining district.

DEFORMATIONAL HISTORY AND STRUCTURE

Large-amplitude Folds

Northeast-trending anticlines and synclines

The structural grain of the district is dominated by sinuous anticlines and synclines that trend to the northeast and appear to be relatively open and upright structures. This structural set is dominated by the Cleary and Gilmore anticlines and the intervening syncline that parallels the valley of Pedro Creek. However, similar structures have also been mapped northwest of the Chatanika River and southeast of the Chena River valleys. Northeast-trending folds appear to wane and disappear further to the southeast in the Yukon-Tanana Upland and are replaced by west- and northwest-trending structures.

The northeast-trending structures appear to represent the most recent deformational episode in the district, because earlier fold axes and mineral lineations frequently plunge off both flanks of the anticlines (Brown, 1962). The elongate geometry of the Pedro Dome and Gilmore Dome plutons also suggests emplacement during the arching of the respective anticlines.

Potassium-argon mineral ages determined for the Pedro Dome plutons (table 1), and greenschist-facies rocks along the trace of the Pedro Dome anticline establish a probable minimum age for the last deformational episode of about 90-120 m.y.

Although the large-scale folds have an apparent open-upright geometry, 'b' mineral lineations parallel to small-scale, northeast-trending, isoclinal recumbent to overturned folds are slightly discordant to the trend of the Pedro Dome anticline (Brown, 1962; Forbes and Weber, 1982, pl. 1).

Smaller scale, northeast-trending folds are also present in the eclogite-bearing terrane, as discussed below.

Northwest-trending recumbent folds and the 'Chatanika Window?'

Although Prindle (1913), Mertie (1937), and Hill (1933) recognized the apparent anticlinal geometry of the structural high that coincides with the axial zone of the 'Cleary anticline' and the Fairbanks mineralized belt, several anomalous relations have long suggested that the structures on the northwest flank of the high were more complicated than those of a simple anticline.

More recent geophysical and petrologic studies (Forbes and others, 1968; Pilkington and others, 1969) revealed that the rather monotonous sequence of micaceous quartzites and quartz-mica schists (± garnet) that had previously defined the axial zone of the Cleary anticline appears to represent a different sequence of crystalline schists that is in thrust and/or apparent fault contact with a fault block or 'window' composed of eclogite-bearing calcium-magnesium rocks, with subordinate pelitic schists and micaceous quartzites. The thrust zone, or fault, between the two sequences is defined by coarse-grained, garnetiferous calc-mylonites (5.5 Mi Elliott highway; Forbes and Weber, 1982, pl. 1) that appear to be cataclastically disrupted and retrograded calc-silicate metamorphic rocks.

The eclogite-bearing sequence is highly contorted, with earliest folding around north- to northwest-trending axes. These folds are characteristically isoclinal recumbent, with the preferred direction of overturning to the southwest. Later folding along northeast-trending axes produced superimposed open folds with axial planes that tend to dip steeply to the southeast. Superposition of these folds upon the earlier isoclinal-recumbent structures also creates culminations and depressions of the earlier fold axes.

A section in the 'c-b' plane of one of the isoclinal folds, when viewed parallel to the tectonic 'a' axis, may appear to be a simple fold rather than a refolded, isoclinal-recumbent structure. This is vividly illustrated in figures 10 and 11. Potassium-argon amphibole ages from the eclogite-bearing terrane indicate that the earliest deformational episode probably occurred no less than 250 m.y. B.P. and perhaps in excess of 450 m.y. B.P. The proposed 450 m.y. minimum age for this event is supported by a 500 m.y. muscovite rubidium-strontium age for schists north of Chatanika by Wasserburg, Eberlein, and Lanphere (1963).

Related microstructures

Microstructures in the greenschist- and amphibolite-facies terrane appear to have been associated with complete recrystallization of the parent rock and the development of metamorphic mineral assemblages that were of higher metamorphic grade than those developed in the later deformation, which appears to have been a retrograde event.

Earlier fold axes are often paralleled by a 'b' lineation defined by biotite, amphibole, or muscovite, and less commonly, sericite. Muscovite or sericite that recrystallized at the time of the second deformation may also define a 'b' lineation locally, which transects the earlier 'b' and parallels the axes of the younger, northeast-trending folds. In some outcrops, the earlier schistosity (S_1) is transected by a later schistosity defined by retrograde sericite or muscovite (S_2).

The polymetamorphic history of the eclogite-bearing terrane is also documented by the microstructures, as seen in the refolding of schistosity and recumbent microfold axial planes. Similar structural relations have been mapped in the field on all scales. The apparent direction of overturning, thinning, and shearing of the overturned limbs of small folds indicates that the principal direction of yielding was to the southwest.

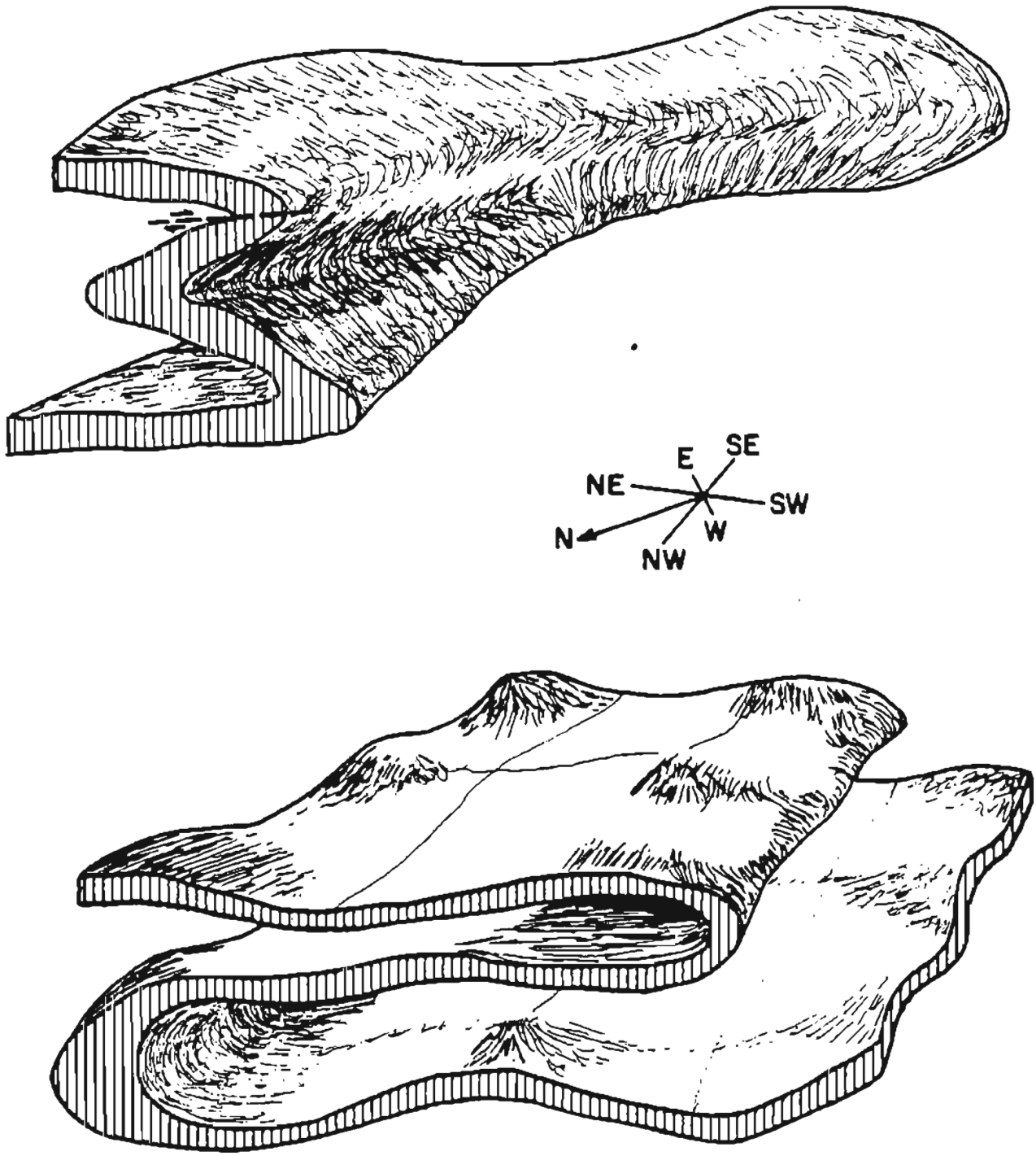

Figure 10. Structural style of folded rocks in the eclogite-bearing terrane, Fairbanks mining district, Alaska.

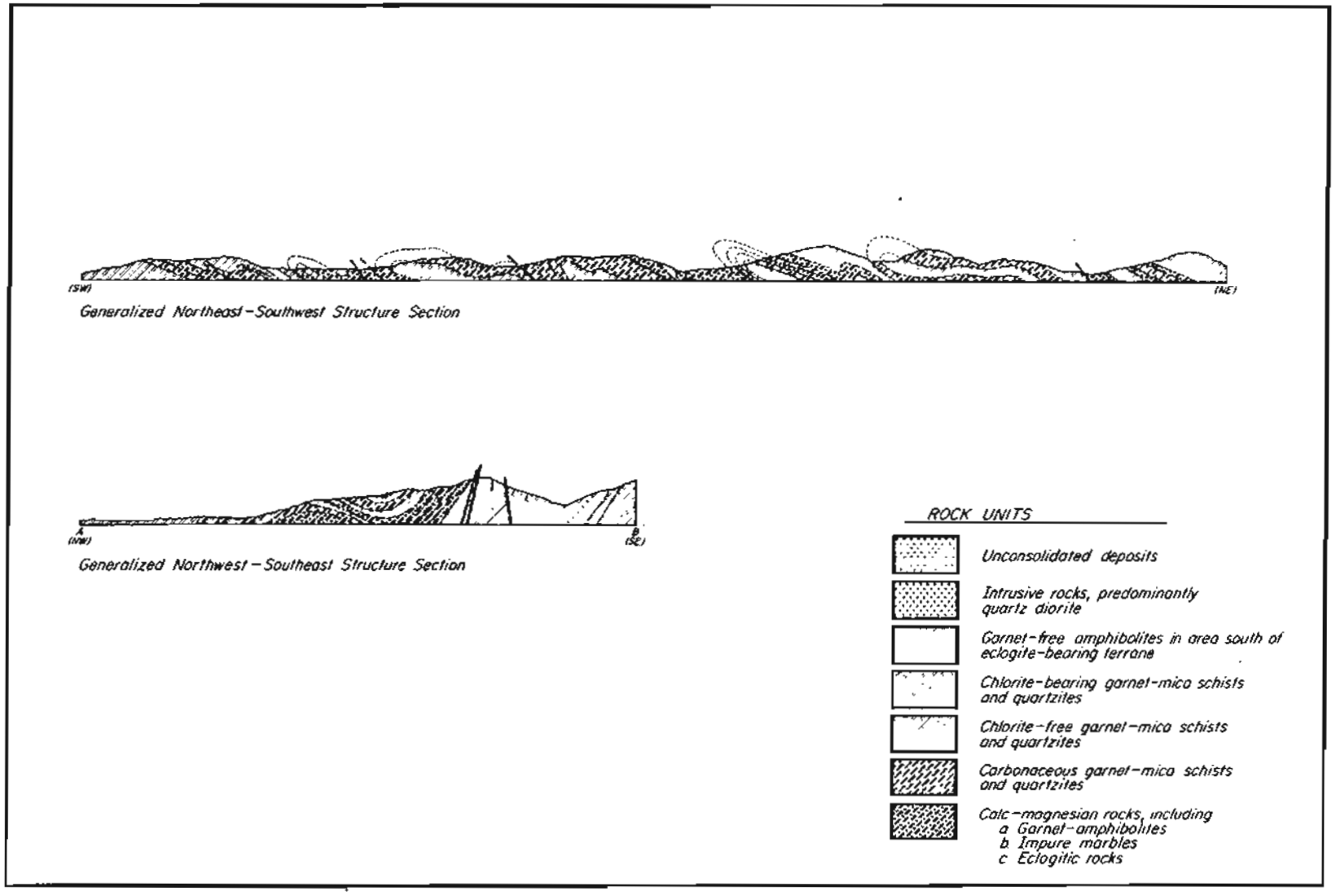

Figure 11. Generalized structure sections across the eclogite-bearing terrane north of Fairbanks, Alaska (Swainbank and Forbes, 1975).

Small-amplitude Folds and Orientation

Small-amplitude folds have been recorded and studied in both terranes. Chevron, subisoclinal, and isoclinal folds occur in the greenschist- and amphibolite-facies terranes. Most folds are overturned or recumbent with yielding to the north. The eclogite-bearing terrane is characterized by isoclinal recumbent folds that reflect the geometry of the large-scale structures.

Stereographic analysis of structural elements in the lower and upper plates

Stereographic plots of measured fold axes and 'b' mineral lineations from pelitic and calc-magnesian variants within the eclogite-bearing terrane show a strong orthorhombic symmetry (fig. 12a) that is in contrast to the monoclinic symmetry shown by a stereographic plot of the structural elements measured in the upper sequence (fig. 12b). The strong northeastern element is apparent in both stereograms, but little suggestion of a northwest trend can be seen in the data recorded in figure 12b.

Eclogite-bearing terrane as a window

Much evidence discussed above suggests that the eclogite-bearing terrane is exposed as a window of more complexly metamorphosed rocks surrounded by an upper-plate sequence of less metamorphosed rocks.

Ester Dome Antiform

Structural measurements, including the attitudes of bedding, foliation, fold axes, and mineral lineations, indicate that the metamorphic rocks of Ester Dome have been deformed into a structural high with the geometry of an asymmetric anticlinorium (fig. 13).

Divergent plunge patterns of small fold axes, with an apex near the topographic summit of Ester Dome, suggest that the structure may actually be an asymmetric dome. Additional evidence for a domal structure is offered by the break in continuity of both rock type and structural axes between Ester Dome and the hills northeast of Goldstream valley. An alternate explanation could be supplied by offset caused by faulting along the trace of the valley, or a combination of doming and faulting.

The amphibolites, coarse-grained garnet-mica schists, and marbles exposed in the Murphy Dome roadcuts on the southwest slope of Goldstream valley have not been found in outcrop or in the subsurface mine workings on Ester Dome. However, this sequence of rocks does occur along the crest of Chena Ridge, south of the Ester-Cripple Creek valley.

Faults

Pedro Dome thrust fault

The eclogite-bearing and greenschist-facies terranes are separated by a deduced thrust(?) fault. Evidence for the geometry and existence of this fault includes:

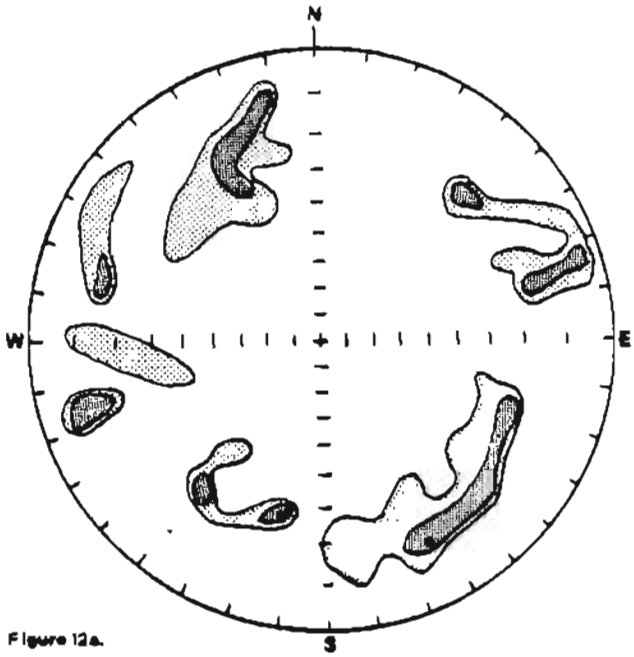

Figure 12a.

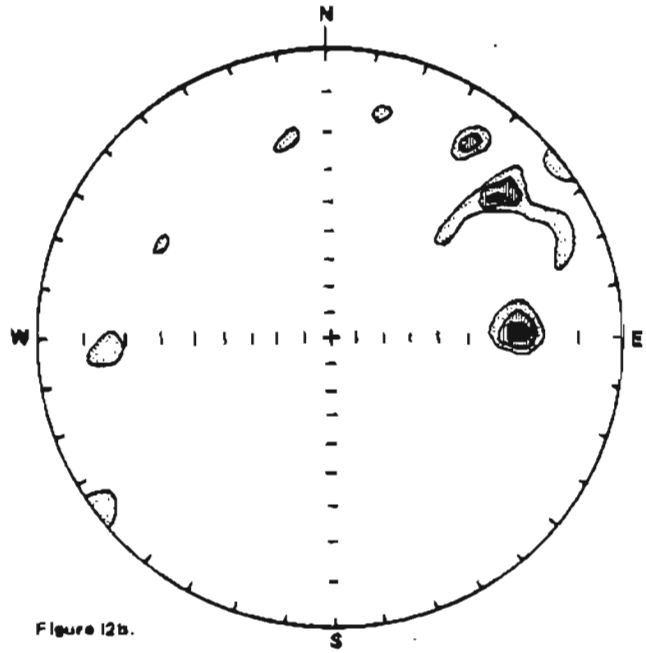

Figure 12b.

Figure 12a) Lower-hemisphere stereographic plot of fold axes and 'b' mineral lineations in the eclogite-bearing terrane, Fairbanks mining district, Alaska. Contours at 4-, 6-, and 8-percent intervals for 175 plots (Swainbank and Forbes, 1975). b) Lower-hemisphere stereographic plot of fold axes and 'b' mineral lineations in the greenschist-facies rocks of the Cleary-Pedro area, Fairbanks mining district, Alaska. Contours at 4-, 6-, and 8-percent intervals for 78 plots (Swainbank and Forbes, 1975).

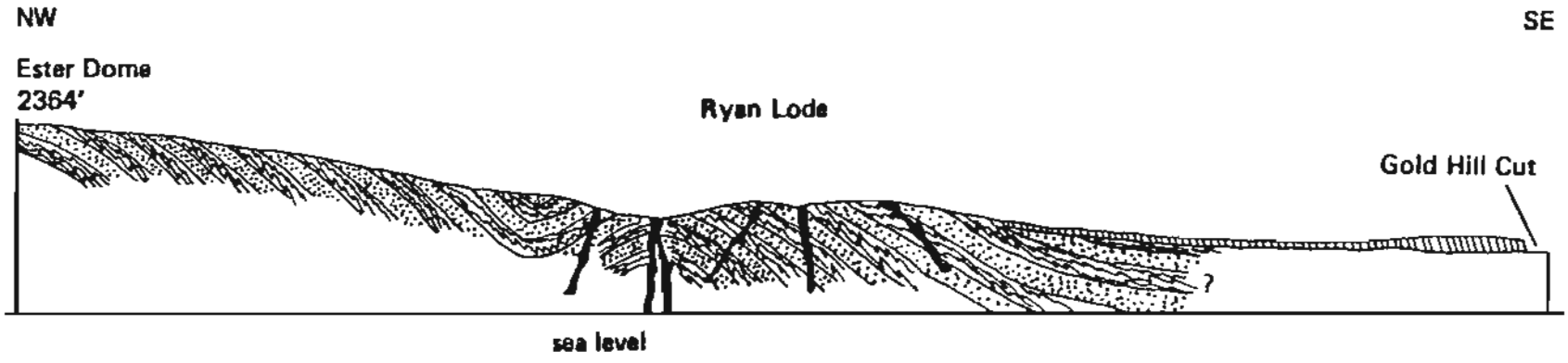

Figure 13. Generalized northwest-southeast structure section across the southeast quadrant of Ester Dome, Alaska. Discordant (black), gold-bearing quartz veins are shown cutting the folded micaceous quartzites, quartz-mica schists, and subordinate calc-magnesian rocks. Northeast-trending open folds, as shown in this section are somewhat misleading, because earlier isoclinal-recumbent folds have been refolded into these apparently simple structures.

.Mylonite zone in the eclogite-bearing sequence, overlain by highly contorted greenschist-facies rock units (Elliott Highway section).
.Abrupt increase in metamorphic grade and lithology from greenschist to amphibolite facies.
.Low-angle, reverse-fault geometry suggested by outcrop patterns in re-entrant valleys on the west flank of Pedro Dome.

Figure 14 illustrates a possible interpretation of these relations, based on the premise that the eclogite- and amphibolite-facies rocks compose a coherent plate that has been thrust over the greenschist terrane and refolded during a subsequent deformational episode.

Dome Creek fault

A major fault zone mapped south of Dome Creek by Brown (1962) trends N. 70° E. and dips 50° SE. The fault zone is approximately 100 ft wide and contains several slices of altered, iron-stained schist. Much blue-gray gouge is present, and the foot and hanging walls are highly stained with iron oxide. A series of step faults with displacements of 3 to 12 in. occurs approximately 50 ft north of the major fault zone. These step faults are high-angle reverse faults that parallel the major fault zone. This is interpreted to indicate that the major fault is also a high-angle reverse fault. Total displacement along this fault is not known. Swainbank (1971) also mapped a northeast-trending, high-angle normal fault in bedrock exposed in a placer cut at the head of Dome Creek.

Clear Creek and Ruby Creek faults

Based on field mapping by Swainbank (1971), inferred high-angle faults appear to parallel the valleys of Cleary and Ruby Creek (Forbes and Weber, 1982, pl. 1). The amount of separation along these faults is not known, but the displacement probably involves movement in both dip-slip and strike-slip components.

Subsurface faulting and mineralization

A review of published reports describing mine workings shows that the schists in the Pedro Dome-Cleary and Ester Dome areas have been extensively faulted. Hill (1933) presented the most complete published data concerning attitudes of faults in both areas (fig. 15).

Figure 16 summarizes Hill's information on fault attitudes for the Pedro Dome-Clear area. The pronounced maximum (fig. 16, sector 1) strikes N. 70° W. This fault set is described by Hill as 'the major post-mineralization faulting...has a west-northwest trend parallel to the trend of the mineralization.' The subordinate maximum (sector 2) indicates a fault set that strikes N. 10° E. Most other faults in the area strike east-west, with the exception of a minor fault set that strikes N. 45° E.

A comparison of figures 15 and 16 indicates that three of the four joint sets prevalent in the schists are also paralleled by the fault sets. The parallelism indicates that the fault and joint systems are probably both

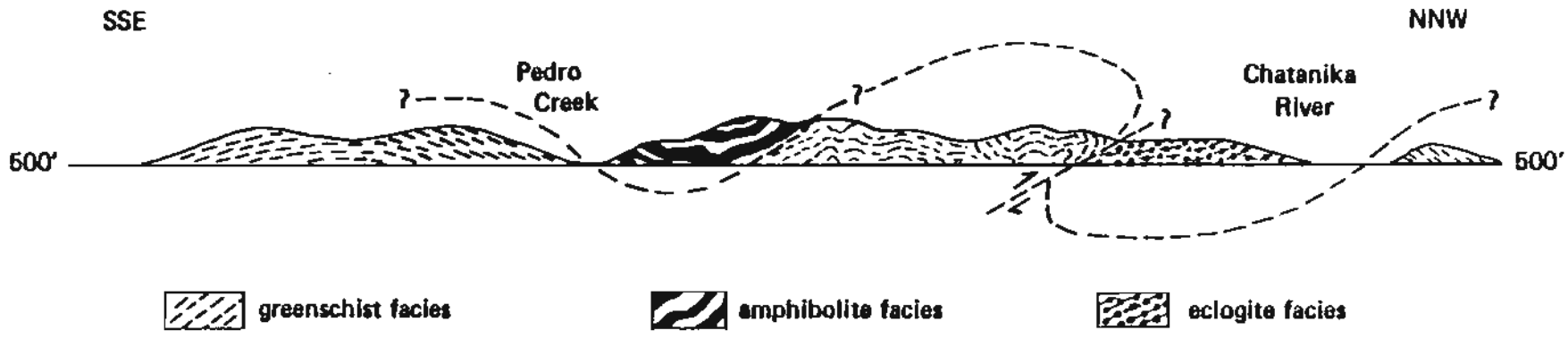

Figure 14. Diagrammatic south-southeast-north-northwest structure section from Gilmore Dome to the Chatanika River valley, Alaska with a structural interpretation based on the assumption that the amphibolite- and eclogite-facies rocks constitute a coherent terrane that has been thrust over a greenschist-facies autochthon, with subsequent folding of the thrust plane during the deformational episode that produced the northeast-trending folds in the district.

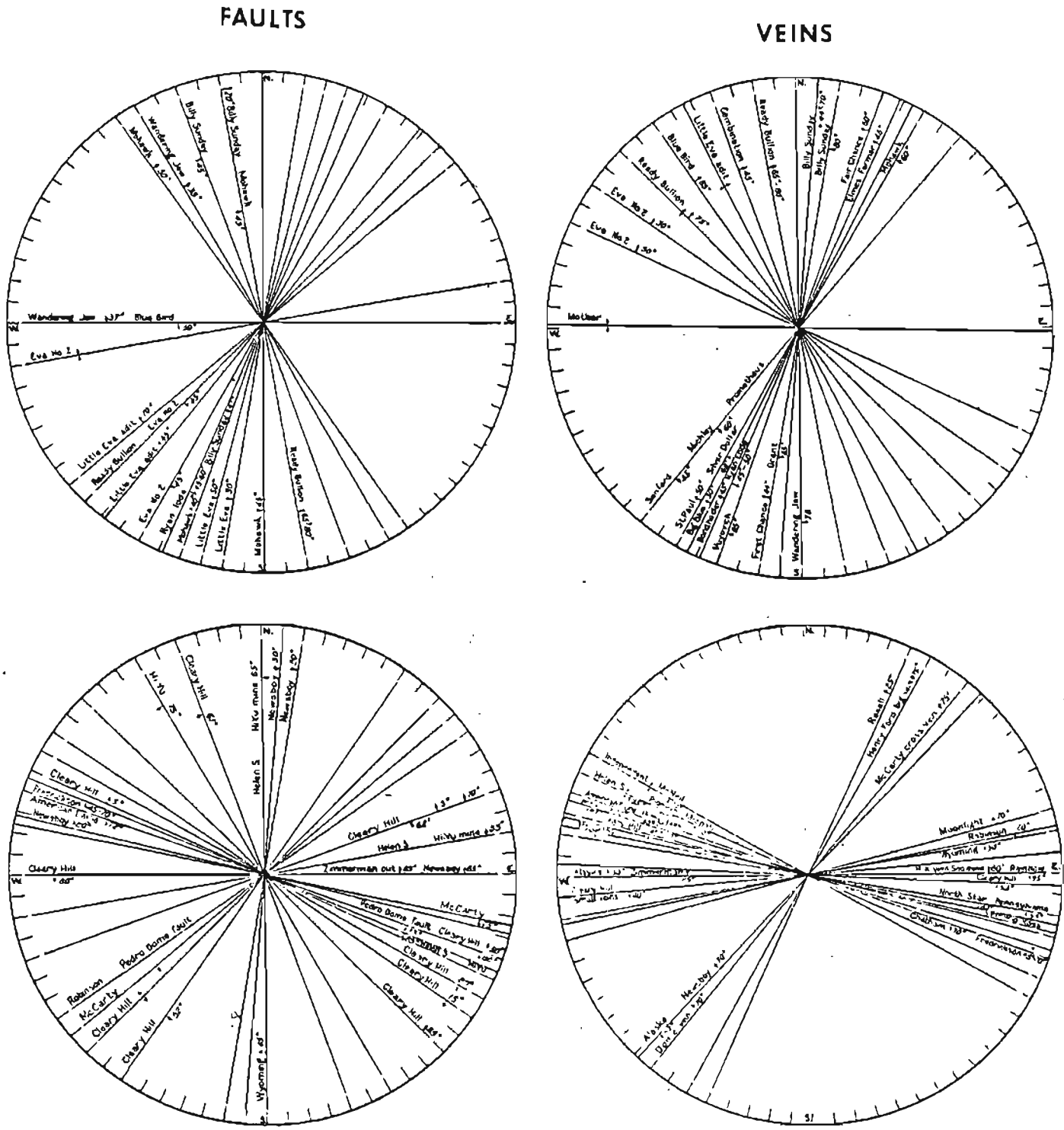

Figure 15. Attitudes of faults and mineralized veins in the Ester Dome (upper) and Pedro Dome-Cleary (lower) areas (Hill, 1933), Fairbanks mining district, Alaska.

related to the anisotropy produced by the structure of the schists. These three fault systems (sectors 1-3, fig. 16) strike N. 70° W., N. 10° E., and N. 45° E., respectively. The joint set that strikes N. 25° W. is apparently not paralleled by a well-developed fault set, although a few parallel faults do occur (sector 4, fig. 16).

Nearly all mineralized lodes in the Pedro Dome-Cleary area are fissure vein fillings formed by deposition along fault zones. Brecciation, slickensides, and gouge indicate recurrent movements along these fault zones. The mineralized faults may be grouped into two sets; the dominant fault set (sector 1, fig. 16) strikes N. 70° W and dips steeply to the southwest, while the other mineralized fault set strikes N. 50° E. and dips steeply to the southeast. The dominant vein system intersects the axis of the Cleary anticline at 30°-40°, while the subordinant system is subparallel to the axis of the Cleary anticline. The fault set that strikes N. 10° E. (sector 2, fig. 16) has apparently not been mineralized.

Investigations of the Vetter-Sheldon property (Kawalita lode) disclosed that the gold-stibnite-quartz vein is offset by a set of parallel faults that trends N. 40° E. and dips 75° SE. The total apparent displacement along these faults is small, on the order of 1 to 3 ft. Observed separation of the vein indicates that the faults may be normal. On Ester Dome, subsurface faulting tends to parallel the orientation of the gold-bearing quartz-lode systems (northwest to northeast sector). The fault zones dip in both easterly and westerly directions and generally exceed 40°. Fault movement and brecciation is associated with mineralization along some vein systems, including the Ryan lode.

INTERPRETATION OF GEOPHYSICAL-SURVEY DATA

Airborne Magnetometer Surveys

Three airborne magnetometer surveys that include part, or all of the Fairbanks mining district are: 'An aeromagnetic reconnaissance of the east-central Tanana Lowland, Alaska' (two maps at 1:125,000 scale), by Andreasen and others, 1964; 'Geologic interpretation of reconnaissance aeromagnetic survey of northeastern Alaska' (1:1,000,000 scale), by Brosgé and others, 1970; and 1:63,360-scale survey of the Fairbanks district that was done under contract to DGGS.

Anomaly patterns on these maps reinforce the presence of a dominant northeast structural grain in the district, accentuated by 200-400 gamma linear anomalies that correlate with amphibolite layers in the amphibolite- and eclogite-facies terranes. In these surveys, grid spacing was apparently too large to provide the resolution required for the recognition of fault offsets and other structural detail.

Surface Gravity and Magnetometer Surveys

Magnetometer profiles

A roadside magnetometer profile was completed with a vertical-component fluxgate magnetometer along the Elliott Highway from Fox to the Chatanika

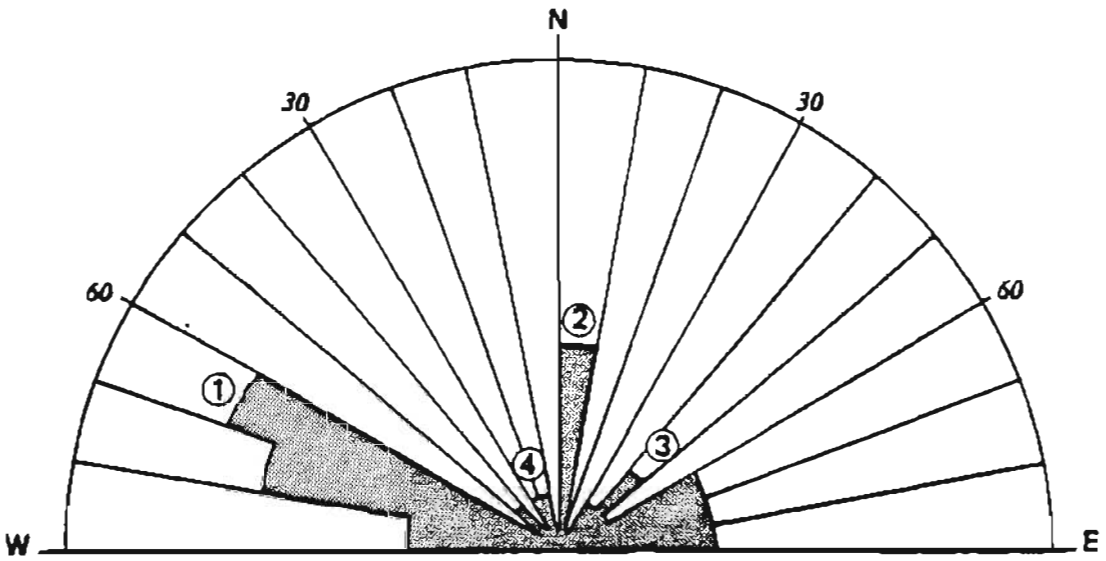

Figure 16. Strike-frequency diagram of faults in the Pedro Dome area, Fairbanks mining district, Alaska, based on data from Hill (1933). Circled numbers refer to discussion in text.

River Bridge, (Forbes and Weber, 1982, pl. 2). Readings were taken at 100-ft intervals, and the magnetometer was held approximately 3 ft above the surface. Data are believed to be significant in the ±20-gamma range.

The Fox-Chatanika River profile parallels the structural section in Forbes and Weber (1982, pl. 1) and the schematic section shown in this report (fig. 11). This profile is characterized by a gradual rise in background toward the northwest and contrasting magnetic signatures for the eclogite and amphibolite-facies terranes vs the greenschist-facies terrane. The eclogite- and amphibolite-facies terranes produce irregular traces with sharp highs caused by intercalated amphibolites and rocks of lower magnetic susceptibility, whereas the greenschist-facies terrane produces a rather subdued trace with small variations, based on the rather monotonous lithology dominanted by quartz-mica schists, micaceous quartzites, and rare calc-schists.

As noted on the airborne magnetic maps, magnetometer surveys provide an excellent technique for mapping and delineating the amphibolite-bearing terranes and the individual amphibolite units.

Gravity profile

A reconnaissance gravity profile (based on 22 stations measured with a Worden gravimeter by Juergen Kienle, Geophysical Institute, University of Alaska) was also completed along the Fox-Chatanika River section. The results of the survey are plotted with a structure section as compiled along the traverse (Forbes and Weber, 1982, pl. 2). All Bouguer values were negative, and the profile is characterized by low values under the axis of the Cleary-Pedro anticline, which is cored by a thick section of greenschist-facies rocks; values increase toward the eclogite- and amphibolite-facies terranes. The gradual increase toward the deduced thrust fault to the northwest reinforces the low-angle geometry of the contact between the two terranes.

MINERALIZED ZONES AND VEIN SYSTEMS

Lode Classification and Distribution

Although this report is directed toward geology, structure, and petrology rather than mineral deposits, a few comments on the interrelationship between petrology, structure, trace chemistry, and anomalous metals concentrations seems to be in order.

The occurrence of gold-bearing quartz lodes defines the Fairbanks gold belt that extends northeast from Ester Dome to Pedro Dome and the Cleary Summit area (Forbes and Weber, 1982, pl. 1). Although contact metasomatic mineral deposits occur along the margins of the quartz monzonite plutons on Gilmore and Pedro Domes, and fissure sulfide veins were encountered in the Busty Belle adit on Pedro Dome, lode deposits in the Fairbanks gold belt are dominantly fissure- or fault-controlled metalliferous quartz veins in micaceous quartzites and quartz-mica schists. Recent work also suggests that strata-bound sulfide concentrations that were formerly interpreted as replacement deposits also occur in the Pedro Dome-Cleary Summit area (Paul Metz, personal commun.).

Although the lode deposits appear to be spatially related to granitic stocks and dikes in the Pedro Dome-Cleary area, this association is not obvious on Ester Dome, unless the plutons are undetected in the subsurface.

Mineralogy of the Gold-bearing Lodes

Sandvik (1967), progressing beyond the earlier work of Hill (1933), determined that the 'introduction of vein minerals took place in four phases, each preceded by tectonic activity which prepared the ground for the passage of hydrothermal solutions.' Sandvik's proposed sequence of mineralization is shown below.

Phase 1 - Quartz (barren of metallic minerals)
Phase 2 - Quartz, loellingite, arsenopyrite, pyrite, and gold
Phase 3 - Quartz, pyrite, gold, sphalerite, chalcopyrite, freibergite, jamesonite, galena, boulangerite, robinsonite, zinkenite, and stibnite
Phase 4 - Quartz and stibnite

Following Lindgren's depth-temperature classification, Phases 1 and 2 are high-temperature mesothermal, Phase 3 is low-temperature mesothermal, and Phase 4 is epithermal.

Sandvik's classification was based on an analysis of recognized lode systems and the paragenesis of vein mineral assemblages. His work did not deal with contact metasomatic mineral deposits or the possibility of strata-bound ore deposits.

Structural Control

As discussed above, there is a correlation between joint sets and faults, and lode orientation. In the Pedro Dome-Cleary area, density of lode deposits appears to be increased along culminations and depressions along the crest of the Pedro-Cleary anticline. On Ester Dome, lodes seem to be concentrated along a cross-warp that appears to be superimposed on the northeast-trending antiform.

We do not understand, however, why there is an apparent barren zone that extends from the Scrafford stibnite deposit southwest to Ester Dome, and separates the two segments of the mineralized belt.

Syngenetic(?) Metals Concentrations vs Secondary Mineralization

An increasing amount of evidence suggests that some rock units in the greenschist-facies terrane are selectively enriched in heavy metals above normal background levels, and that the origin of these concentrations may be syngenetic rather than by secondary alteration and/or chemical replacement. For example, auger and grab samples of bedrock along the Ester Dome road traverse (Stevens and others, 1969) produced anomalous gold, arsenic, and antimony values---across a very wide zone on trend with the Ryan lode---which was not associated with a high density of mineralized lodes. Similar anomalies were encountered in grab and channel samples in a wide zone cut by the Elliott Highway from Fox to Olnes, adjacent to the crest of the Pedro-Cleary antiform (Hawkins and Forbes, 1971). Additionally, studies of arsenic-rich ground water in the district (Hawkins and others, 1982) show that certain rock units cut by water wells on Ester Dome contain relatively high concentrations of arsenic. There is also a correlation between arsenic-bearing aquifers cut by water wells and high levels of arsenic in well water.

Water wells with high arsenic values are found in other areas within the district other than Ester Dome, and some of these areas do not contain known mineralized lodes, which suggests that rock units containing anomalous arsenic and other heavy metals may be present elsewhere in the district, even though lode systems are not known.

The possible significance of these observations is reinforced by the recent findings of Paul Metz and M.S. Robinson (personal commun.), who have discovered previously unrecognized strata-bound scheelite, cinnabar, and other sulfides in Pedro-Cleary area.

UNANSWERED PROBLEMS AND RECOMMENDATIONS FOR FUTURE WORK

Regional Tectonics, Structure, and Geochronology

Geochronology and tectonics

The deformational and recrystallization history of the metamorphic rocks, including the age and provenance of the rocks composing the protolith, is poorly understood. Potassium-argon dating work has shown that other radiometric dating techniques, including rubidium-strontium and uranium-lead methods, must be applied to the problem to solve the age relations of the parental sedimentary rocks (and their source terranes) and the succeeding metamorphic and/or deformational events.

Although preliminary structural analyses have identified at least two structural episodes in the district, detailed structural mapping and petrofabrics studies are needed if the interrelationships between structures in the three metamorphic terranes are to be understood.

Structure

The possible interrelationship of the eclogite- and amphibolite-facies metamorphic rocks, as facies variations within a formerly coherent terrane, constitutes a persistent and important problem. Such a relationship requires a folded thrust, with subsequent deformation and faulting. Subsurface data are needed to confirm the possible presence of eclogite- and amphibolite-facies rocks in those areas where they should underlie the greenschist-facies terrane.

Definitive subsurface data could be acquired from test holes at appropriate locations, and detailed geophysical studies, including surface and airborne magnetometer surveys and gravity profiles along selected traverses, could be conducted.

Petrology

Eclogite-facies terrane

Earlier work has confirmed the eclogitic rocks as true eclogites vs skarns, rodingites, or diopside-bearing calc-garnet schists. What is not at all clear, however, is why the pelitic rocks do not contain equilibrium assemblages with the kyanite that appears to be in the required pressure-temperature field. As mentioned previously, relict kyanite and staurolite(?) were found in one rock sample near the old Cleary townsite. It is possible that kyanite-bearing assemblages may have been obliterated by the pervasive Jurassic and/or Cretaceous thermal overprints.

Careful sampling of pelitic variants in the eclogite-facies terrane is recommended. Many calc-magnesian units within this terrane have not been adequately sampled and studied.

Amphibolite- vs greenschist-facies terranes

Although the comparative metabasite assemblages in the two terranes appear to be definitive (e.g., hornblende-oligoclase-epidote-sphene ± biotite, garnet, rutile vs actinolite-albite-epidote-chlorite-sphene), and other characteristic units, including gneisses, are not known to occur in the rocks now considered to constitute the greenschist terrane, some questions remain:

- What is the detailed mineralogy of the assemblages in the rather rare marble units?
- Are the calc-magnesian units mapped on the northwest flank of Gilmore Dome as amphibolite-facies rocks properly identified, or are they actually hornfelsed calc-magnesian units of the greenschist-facies terrane?
- What is the mineralogy and facies assignment of the sulfide-bearing layered marbles in the headwaters of Cleary Creek?
- What was the protolith of feldspathic schists in the greenschist-facies terrane---metaigneous vs metasedimentary?
- What was the tectonic setting, provenance, and clastic source for the metasedimentary rocks of the greenschist terrane?

Granitic rocks

The Gilmore Dome pluton and the skarn assemblages associated with the scheelite deposits need further study. The whole-rock chemistry and preliminary trace-element studies of analyzed granitic rocks indicate that the more siliceous granitic rocks are of anatectic origin, and that they may contain relatively high concentrations of trace metals and indicator elements. This lead should be followed by geochemical studies.

Siliceous (granitic) dike rocks have been inadequately studied. Systematic sampling, petrographic studies, and trace-chemical analyses are needed.

Mineral Deposits

Recent work by MIRL and DGGS geologists indicates that some of the feldspathic schists and calc-schists in the greenschist-facies terrane contain anomalous concentrations of metals, including tungsten, antimony, arsenic, lead, zinc, mercury, and gold. Some concentrations may be of syngenetic and/or volcanogenic origin, and because this possibility carries significant economic implications, it deserves priority study.

We know of no significant lode deposits in the eclogite- or amphibolite-facies terrane. This observation is important, if true, but it must be rechecked in detail.

There appears to be a 'barren zone' devoid of lode mineralization in the greenschist-facies terrane from the area near the head of Vault and Treasure Creeks along the old road to 'Love Site' and Murphy Dome. This is an important gap (if real) and must be reinvestigated, and explained if it survives additional work.

REFERENCES CITED

Aleinikoff, J.N., Dusel-Bacon, Cynthia, Foster, H.L., and Futa, K., 1981, Protozoic zircon from augen gneiss, Yukon-Tanana Upland, east-central Alaska: Geology, v. 9/10, p. 469-473.

Andreasen, G.E., Wahrhaftig, C.A., and Zietz, I., 1964, Aeromagnetic reconnaissance of the east-central Tanana Lowland, Alaska: U.S. Geological Survey Geophysical Investigations Map GP-447.

Berg, H.C., and Cobb, E.H., 1967, Metalliferous lode deposits of Alaska: U.S. Geological Survey Bulletin 1246, 254 p.

Biggar, N.E., 1973, A geological and geophysical study of Chena Hot Springs, Alaska: Fairbanks, University of Alaska unpublished M.S. thesis, 72 p., 3 pl.

Bowen, N.L., 1928, The evolution of igneous rocks: Princeton, New Jersey, Princeton University Press, 332 p.

Brabb, E.E., and Churkin, Michael, Jr., 1969, Geologic map of the Charley River Quadrangle, east-central Alaska: U.S. Geological Survey Miscellaneous Geologic Investigations Map I-573.

Britton, J.M., 1969, Petrology and petrography of the Pedro Dome plutons, Alaska: Fairbanks, University of Alaska unpublished M.S. thesis, 52 p.

Brooks, A.H., 1900, A reconnaissance in the Tanana and White River Basins, Alaska, in 1898: U.S. Geological Survey 20th Annual Report, Part 7, p. 425-494.

Brosgé, W.P., Brabb, E.E., and King, E.R., 1970, Geologic interpretation of reconnaissance aeromagnetic survey of northeastern Alaska: U.S. Geological Survey Bulletin 1271-F, 14 p.

Brown, J.M., 1962, Bedrock geology and ore deposits of the Pedro Dome area, Fairbanks Mining District, Alaska: University of Alaska unpublished M.S. thesis, 137 p.

Byers, F.M., Jr., 1957, Tungsten deposits in the Fairbanks District, Alaska: U.S. Geological Survey Bulletin 1024-I, p. 179-216.

Chapin, T., 1914, Lode mining near Fairbanks: U.S. Geological Survey Bulletin 592, p. 321-356.

Chapman, R.M., and Foster, R.L., 1969, Lode mines and prospects in the Fairbanks District, Alaska: U.S. Geological Survey Professional Paper 625-D, 25 p.

Chapman, R.M., Weber, F.R., and Taber, B., 1971, Preliminary geologic map of the Livengood Quadrangle, Alaska: U.S. Geological Survey Open-file Report 71-66, 2 sheets.

Chappell, B.W., and White, A.J.R., 1974, Two contrasting granite types: Pacific Geology, v. 8, p. 173-174.

Clark, F.W., 1920, The data of geochemistry: U.S. Geological Survey Bulletin 695, 832 p.

Coleman, R.G., Lee, D.E., Beatty. L.B., and Brannock, W.W., 1965, Eclogites and eclogites: Their differences and similarities: Geological Society of America Bulletin, v. 76, p. 483-508.

Forbes, R.B., and Brown, J.M., 1961, Preliminary geologic map of the Fairbanks Mining District, Alaska: Alaska Division of Mines and Minerals Report 194-1.

Forbes, R.B., Pilkington, H.D., and Hawkins, D.B., 1968, Gold gradients and anomalies in the Pedro Dome-Cleary Summit area, Fairbanks District, Alaska: U.S. Geological Survey Open-file Report 68-101, 43 p.

Forbes, R.B., Pulpan, Hans, and Gedney, Larry, 1976, Seismic risk and the Denali fault: Fairbanks, Geophysical Institute, University of Alaska report.

Forbes, R.B., and Weber, F.R., 1975, Progressive metamorphism of schists recovered from a deep drill hole near Fairbanks, Alaska: U.S. Geological Survey Journal of Research, v. 3, no. 6, p. 647-657.

_____, 1982, Bedrock geologic map of the Fairbanks mining district, Alaska: Alaska Division of Geological and Geophysical Surveys Open-file Report 170, scale 1:63,360, 2 pl.

Foster, H.L., 1970, Reconnaissance geologic map of the Tanacross Quadrangle, Alaska: U.S. Geological Survey Miscellaneous Investigations Map I-593.

Foster, H.L., Forbes, R.B., and Ragan, D.M., 1966, Granulite and peridotite inclusions from Prindle Volcano, Yukon-Tanana Uplands, Alaska in Geological Survey Research, 1966: U.S. Geological Survey Professional Paper 575-D, p. D120-D122.

Foster, H.L., and Keith, T.C., 1968, Preliminary geologic map of the Eagle B-1 and C-1 Quadrangles, Alaska: U.S. Geological Survey Open-file Report 68-103.

Foster, H.L., Weber, F.R., Forbes, R.B., and Brabb, E.E., 1973, Regional geology of Yukon-Tanana Upland, Alaska, in Arctic Geology, American Association of Petroleum Geologists Memoir 19, p. 388-395.

Furst, G.A., 1968, Geology and petrology of the Fairbanks basalts, Fairbanks, Alaska: Fairbanks, University of Alaska unpublished M.S. thesis, 53 p.

Griscom, A., 1976, Aeromagnetic map and interpretation of the Tanacross Quadrangle, Alaska: U.S. Geological Survey Miscellaneous Field Studies Map MF-767A.

Hahn-Weinheimer, P., 1960, Bor-und Kohlenstoffgehalte basischer bis intermediarer metamorphite der Munchberger Gneismasse und ihre $^{12}C/^{13}C$-isatopenverhaetnisse: International Geologic Congress, 21st, Copenhagen, part. XIII, p. 431-442.

Hawkins, D.B., and Forbes, R.B., 1971, Investigation of gold mineralization along a part of the Elliott Highway, Fairbanks District, Alaska: U.S. Geological Survey Open-file Report 71-147, 65 p.

Hawkins, D.B., Forbes, R.B., Hok, C.I., and Dinkel, Donald, 1982, Arsenic in the water, soil, bedrock, and plants of the Ester Dome area, Alaska: Fairbanks, University of Alaska Institute of Water Resources Report 103, 81 p.

Hill, J.M., 1933, Lode deposits of the Fairbanks District, Alaska: U.S. Geological Survey Bulletin 849-B, p. 29-163.

Holm, Bjarne, 1973, Bedrock geology of the Mt. Prindle area, Yukon-Tanana Valley, Alaska: Fairbanks, University of Alaska unpublished M.S. thesis.

Holmes, G.W., and Foster, H.L., 1968, Geology of the Johnson River area, Alaska: U.S. Geological Survey Bulletin 1249, 49 p.

Jahns, R.H., and Burnham, C.W., 1957, Preliminary results from experimental melting and crystallization of Harding pegmatite: Geological Society of America Bulletin, v. 68, p. 1751-1752.

MacDonald, G.A., and Katsura, T., 1964, Chemical composition of Hawaiian lavas: Journal of Petrology, v. 5, p. 82-133.

Mertie, J.B., Jr., 1918, Lode mining in the Fairbanks District, Alaska: U.S. Geological Survey Bulletin 662, p. 403-424.

_____, 1937, The Yukon-Tanana region, Alaska: U.S. Geological Survey Bulletin 872, 276 p.

Nockolds, S.R., 1954, Average chemical compositions of some igneous rocks: Geological Society of America Bulletin, v. 65, p. 1007-1032.

Péwé, T.L., 1958, Geologic map of the Fairbanks (D-2) Quadrangle, Alaska: U.S. Geological Survey Geologic Quadrangle Map GQ-110.

_____, 1975, Quaternary geology of Alaska: U.S. Geological Survey Professional Paper 835, 145 p.

Péwé, T.L., Bell, J.W., Forbes, R.B., and Weber, F.R., 1975, Geological map of the Fairbanks (D-2 NW) Quadrangle, Alaska: U.S. Geological Survey Miscellaneous Investigations Map I-907.

_____1976a, Geological map of the Fairbanks (D-2 SW) Quadrangle, Alaska: U.S. Geological Survey Miscellaneous Investigations Map I-829A.

_____, 1976b, Geological map of the Fairbanks (D-2 SE) Quadrangle, Alaska: U.S. Geological Survey Miscellaneous Investigations Map I-947.

_____, 1976c, Geological map of the Fairbanks (D-2 NE) Quadrangle, Alaska: U.S. Geological Survey Miscellaneous Investigations Map I-950.

Péwé, T.L., and Holmes, G.W., 1964, Geology of the Mt. Hayes (D-4) Quadrangle, Alaska: U.S. Geological Survey Miscellaneous Investigations Map I-394.

Péwé, T.L., and Rivard, N.R., 1961, Geologic map and section of the Fairbanks (D-3) Quadrangle, Alaska: U.S. Geological Survey Miscellaneous Investigations Map I-340.

Péwé, T.L., Wahrhaftig, Clyde, and Weber, F.R., 1966, Geologic map of the Fairbanks Quadrangle, Alaska: U.S. Geological Survey Miscellaneous Investigations Map I-455.

Pilkington, H.D., Forbes, R.B., Hawkins, D.B., Chapman, R.M., and Swainbank, R.C., 1969, Preliminary investigation of gold mineralization in the Pedro Dome-Cleary Summit area, Fairbanks District, Alaska: U.S. Geological Survey Open-file Report 69-206, 47 p.

Plafker, George, Hudson, Travis, Bruns, T., and Rubin, M., 1978, Late Quaternary offsets along the Fairweather Fault and crustal plate interactions in southern Alaska: Canadian Journal of Earth Science, v. 15, no. 5, p. 805-816.

Prindle, L.M., 1905, The gold placers of the Fortymile, Birch Creek, and Fairbanks regions: U.S. Geological Survey Bulletin 251, 89 p.

_____, 1906, Yukon placer fields: U.S. Geological Survey Bulletin 284, p. 109-131.

_____, 1906, The Yukon-Tanana region, Alaska: Description of the Circle Quadrangle: U.S. Geological Survey Bulletin 295, 27 p.

_____, 1908, Occurrence of gold in the Yukon-Tanana region: U.S. Geological Survey Bulletin 345, p. 179-186.

_____, 1910a, Sketch of the geology of the northeastern part of the Fairbanks Quadrangle: U.S. Geological Survey Bulletin 442, p. 203-209.

_____, 1910b, Auriferous quartz veins of the Fairbanks district: U.S. Geological Survey Bulletin 442, p. 210-229.

_____, 1913, A geologic reconnaissance of the Fairbanks Quadrangle, Alaska: U.S. Geological Survey Bulletin 525, 220 p.

Prindle, L.M., Hess, F.L., and Covert, C.C., 1908, The Yukon-Tanana region, Alaska: Description of the Fairbanks and Rampart Quadrangles: U.S. Geological Survey Bulletin 337, 102 p.

Prindle, L.M., and Katz, F.J., 1909, The Fairbanks gold-placer region: U.S. Geological Survey Bulletin 379, p. 181-200.

Richter, D.H., 1976, Geologic map of the Nabesna Quadrangle, Alaska: U.S. Geological Survey Map I-932.

Roddick, J.A., 1967, Tintina trench: Journal of Geology, v. 75, p. 23-32.
Sandvik, P.O., 1964, Metal distribution in ore deposits of central Alaska: Stanford, California, Stanford University, unpublished Ph.D. thesis, 144 p.
_____, 1967, Mineralogy and distribution of metallic minerals in the Fairbanks District, Alaska: Alaska Centennial Minerals Conference, AIME, unpublished.
Smith, P.S., 1913, Account of lode mining near Fairbanks: U.S. Geological Survey Bulletin 525, 220 p.
Smulikowski, K., 1964, An attempt at eclogite classification: Bulletin de l'Academie Polonaise des Sciences, Serie des Sciences Geologiques et Geographiques, v. 12, no. 1, p. 27-33.
_____, 1965, Chemical differentiation of garnets and clinopyroxene from eclogites: Bulletin de l'Academie Polonaise des Sciences, Serie des Sciences Geologiques et Geographiques, v. 13, p. 11-18.
Spurr, J.E., 1898, Geology of the Yukon gold district, Alaska: U.S. Geological Survey 18th Annual Report, part 3, p. 87-392.
Stevens, D.L., Forbes, R.B., and Hawkins, D.B., 1969, Gold anomalies and magnetometer profile data, Ester Dome area, Fairbanks, Alaska: U.S. Geological Survey Open-file Report 69-266, 43 p.
Stone, R.W., 1906, Reconnaissance from Circle to Fort Hamlin: U.S. Geological Survey Bulletin 284, p. 128-131.
Swainbank, R.C., 1971, Geochemistry and petrology of eclogitic rocks in the Fairbanks District, Alaska: Fairbanks, University of Alaska unpublished Ph.D. thesis.
Swainbank, R.C., and Forbes, R.B., 1975, Petrology of eclogitic rocks from the Fairbanks District, Alaska: Geological Society of America Special Paper 151, 7 p.
Wasserburg, G.J., Eberlein, G.D., and Lanphere, M.A., 1963, Age of Birch Creek schist and some batholithic intrusions in Alaska: Geological Society of America Special Paper 73, p. 258-259.
Weber, F.R., Foster, H.L., and Keith, T.E.C., 1977, Reconnaissance geologic map of the Big Delta (A-2 and A-3) Quadrangles, Alaska: U.S. Geological Survey Miscellaneous Field Studies Map MF-869.
Weber, F.R., Hamilton, T.D., Hopkins, D.M., Repenning, C.A., and Haas, H., 1981, Canyon Creek: A late Pleistocene vertebrate locality in interior Alaska: Quaternary Research, v. 16/2, p. 167-180.
Wilson, F.H., 1976, Map showing potassium-argon ages from the Big Delta Quadrangle, Alaska: U.S. Geological Survey Open-file Report 76-436.
Wilson, F.H., and Shew, Nora, 1981, Map and tables showing preliminary results of potassium-argon age studies in the Circle Quadrangle, Alaska, with a compilation of previous dating work: U.S. Geological Open-file Report 81-889, 1 sheet, scale 1:250,000.